NTNU – Trondheim
Norwegian University of
Science and Technology

# Dynamic Positioning in Extreme Sea States

*Improving Operability Using Hybrid Design Methods*

Astrid Helene Brodtkorb

Marine Technology
Submission date: May 2014
Supervisor: Asgeir Johan Sørensen, IMT
Co-supervisor: Anne Marthine Rustad, IMT

Norwegian University of Science and Technology
Department of Marine Technology

NTNU - Trondheim
Norwegian University of Science and Technology
*Department of Marine Technology*

---

Master Thesis

# Dynamic Positioning in Extreme Seas

*Improving Operability Using Hybrid Design Methods*

---

Astrid H. Brodtkorb

$30^{th}$ of May 2014

Supervisor: Professor Asgeir J. Sørensen
Co-supervisor: Associate Professor Anne Marthine Rustad

**NTNU Trondheim**
**Norwegian University of Science and Technology**
*Department of Marine Technology*

**MASTER THESIS IN MARINE CYBERNETICS**

**Spring 2014**

**FOR**

**STUD. TECH. Astrid H. Brodtkorb**

# Dynamic Positioning in Extreme Sea States

## Work description

Oil and gas exploration and production activities are currently venturing into deeper waters resulting in an increasing number of subsea installations at the sea bed. Vessels with dynamic positioning (DP) capabilities are high in demand both due to their flexibility and good abilities to keep their position with high accuracy. With growing operational costs it is important that vessels on site can conduct operations even in harsher environmental conditions, thereby maximizing the operational window.

The aim of this thesis is to evaluate the performance of high-level hybrid DP algorithms in extreme seas. This work is a continuation of the candidate's previous work. This master thesis should consist of two scientific papers, with a resume. The first paper should look at a hybrid DP controller in a varying sea state, and the second paper should look at a hybrid observer concept designed to cope with noisy measurements.

## Scope of work

Resume:

- Describe the DP concept and the associated operational challenges.
- Review relevant literature related to hybrid systems, model-based and sensor-based observers, and DP in extreme sea states.
- Describe hybrid systems framework proposed by Sanfelice, Goebel and Teel.

Paper one:

- Dynamic positioning from calm to extreme seas using a hybrid controller.
- Design and stability analysis of hybrid controller using framework proposed by Sanfelice, Goebel and Teel.
- Simulate using Matlab/Simulink MCSim simulator, and discuss results.

Paper two:

- Hybrid observers designed using framework proposed by Sanfelice, Goebel and Teel.
- Observer 1 for non-noisy measurements, and observer 2 for noisy measurements.
- Simulate each observer in Matlab/Simulink, and compare performance.

**NTNU Trondheim**
**Norwegian University of Science and Technology**
*Department of Marine Technology*

The report shall be written in English and edited as an article collection with a resume in front, in the format of a report. It is supposed that Department of Marine Technology, NTNU, can use the results freely in its research work, unless otherwise agreed upon, by referring to the student's work. The thesis should be submitted by June 30th 2014.

Co-supervisor: Associate Professor Anne Marthine Rustad

Professor Asgeir J. Sørensen
Supervisor

# Abstract

This thesis investigates the performance of high-level hybrid dynamic positioning (DP) algorithms in extreme environmental conditions. A vessel in DP uses the thrusters as the sole means of keeping position in wind, waves and current, giving both flexible and accurate position keeping. Therefore vessels with DP capabilities are high in demand in industries like for instance the offshore, aquaculture, renewable energy industries and emerging fields like offshore mining. Due to high day rates the focus today is on developing DP systems for extending the operational window to even harsher environments, while keeping the solutions safe and environmentally friendly.

When a sea state transitions from calm to extreme, the wind velocities increase generating higher and longer incident waves. This makes both horizontal and vertical relative motions of the vessel larger with longer periods of oscillation, which has consequences for the DP system onboard. Given the nature of a transitioning sea state, hybrid design methods are used to design a controller and an observer concept.

A hybrid controller, for a vessel in a varying sea state is designed, and global asymptotic stability is established. Simulations in a sea state varying from calm to extreme are conducted with the hybrid controller, consisting of four candidate controllers, and a single controller with adaptive wave filtering for comparison. The single controller becomes unstable in extreme seas whereas the hybrid controller shows good performance. Candidate controllers are selected based on spectral analysis of the vessel wave frequency motions.

A simplified sensor-based hybrid observer concept is investigated for noise robust position estimation. The concept assumes that acceleration measurements are readily available, and can be integrated to obtain position estimates. Position measurements are taken occasionally, and at these instances the position estimate is updated. Stability of the concept is analyzed giving uniform global asymptotic stability, and the simulation of two one degree of freedom sensor-based hybrid observers which rely on acceleration, velocity and position measurements is conducted.

# Sammendrag

Denne masteroppgaven bruker hybride designmetoder til å utforme kontrollalgoritmer for fartøyer som ligger i dynamisk posisjonering i ekstreme sjøtilstander. Hensikten er å vurdere om disse metodene kan biddra med å øke operasjonsvinduet til fartøyet, slik at marine operasjoner ikke er like væravhengige som i dag. Et fartøy i DP bruker thrustere som eneste middel for å holde posisjonen i vind, bølger og strøm, noe som både er fleksibelt og gir nøyaktig posisjonering. Derfor er fartøy med DP system høyt etterspurt i en rekke områder som for eksempel offshore olje og gass, havbruk, fornybar energi, og nyere industri som offshore gruvedrift. På grunn av høye dagrater er fokus i dag å utvikle DP-systemer for å øke operasjonsvinduet til enda vanskeligere miljøer, samtidig som at løsningene forblir sikre og miljøvennlige.

Når en sjøtilstand endres fra rolig til ekstrem, øker vindstyrken med kast som genererer lengere og høyere bølger enn normalt. Dette fører til at både de horisontale og vertikale bevegelsene til fartøyet øker, og endrer mye av fysikken i systemet. Dette får konsekvenser for strukturen til kontrollalgoritmene i DP-systemet ombord. I dette arbeidet er hybride designmetoder brukt til å utforme en hybrid kontroller og en estimator

En hybrid kontroller for et DP-fartøy i en varierende sjøtilstand er utformet, og global asymptotisk stabilitet er etablert. Simuleringer er gjort av et fartøy i en sjøtilstand som varierer fra rolig til ekstrem med to forskjellige kontrollere for sammenligning av ytelse. Den ene er den hybride kontrolleren, med fire underkontrollere valgt basert på estimat av sjøtilstanden, og den andre er en enkelt kontroller med adaptiv bølgefiltrering for sammenligning. Den adaptive kontrolleren blir ustabil i ekstrem sjø, mens den hybride kontrolleren har god ytelse.

En forenklet estimator basert på målinger med støy er utviklet for robust positionsestimering. Konseptet antar at kontinuerlige akselerasjonsmålinger er tilgjengelige, og at de kan integreres to ganger for å oppså posisionsestimater. Måling av den eksakte posisjonen gjøres av og til, og da blir posisjonsestimatet oppdatert. Estimatoren er uniform global asymptotisk stabil, og simuleringer av to versjoner av konseptet er gjort i en frihetsgrad.

# Preface

This master thesis is written during the spring 2014 as the final part of the master program at the department of Marine Technology at the Norwegian University of Science and Technology (NTNU) in Trondheim.

This work is a part of research project 7 *Autonomous marine operations in extreme seas, violent water-structure interactions, deep waters and Arctic* at the Centre for Autonomous Marine Operations and Systems (AMOS).

The thesis is edited as a collection of scientific papers with a resume in front. The first paper with title *Increasing the Operation Window for Dynamic Positioned Vessels Using the Concept of Hybrid Control* is to be published at the *ASME 2014 33$^{rd}$ International Conference on Ocean, Offshore and Arctic Engineering, OMAE 2014*, and the second paper with title *Sensor-Based Hybrid Observer for Dynamically Positioned Vessels* is submitted to the *2014 IEEE Multi-conference on Systems and Control, (MSC)*.

Until the papers are published, this thesis is for Limited circulation.

# Acknowledgments

Thanks to my supervisor Professor Asgeir J. Sørensen, co-supervisor Associate professor Anne Marthine Rustad, and co-author on both the papers Professor Andrew R. Teel for their contributions to this master thesis. Asgeir is a continuous source of inspiration, always giving great advice on marine control and on life in general. Anne Marthine has patiently read through every sentence in this work multiple times, commenting on sentence structure, readability and theory. Andrew inspired me to pursue hybrid control in the first place, and has been answering emails on hybrid modeling and stability analysis with enthusiasm. You have all been vital for the contents of this thesis.

Trondheim, $30^{th}$ of May 2014

Astrid H. Brodtkorb

# Acronyms and Symbols

The most important acronyms and symbols used in the thesis, excluding the papers, are listed here. They are also defined when first introduced.

| | |
|---|---|
| AFB | Acceleration feedback |
| CPM | Control plant model |
| DOF | Degree(s) of freedom |
| DP | Dynamic positioning |
| GNSS | Global navigation and sensor system |
| HiPAP | High precision acoustic positioning system |
| IMU | Inertial measurement unit |
| JONSWAP | Joint North Sea Wave Project |
| NED | North-East-Down reference frame |
| NPO | Nonlinear passive observer |
| OSC | Outer semicontinuous |
| PID | Proportional, integral, derivative gain controller structure |
| PPM | Process plant model |
| PSV | Platform supply vessel |
| RAO | Response amplitude operator |
| UGAS | Uniformly globally asymptotically stable |

Lowercase bold symbols denote vectors, uppercase bold symbols denote matrices, and non-bold italic symbols denote scalars.

*Hydrodynamic coefficients*

| | |
|---|---|
| $\mathbf{M}$ | Inertia matrix including added mass |
| $\mathbf{C}_{RB}(\boldsymbol{\nu})$ | Rigid body Coriolis matrix |
| $\mathbf{C}_{A}(\boldsymbol{\nu}_r)$ | Added mass Coriolis matrix |
| $\mathbf{D}(\boldsymbol{\kappa}, \boldsymbol{\nu}_r)$ | Damping matrix including linear and nonlinear terms |
| $\boldsymbol{G}(\boldsymbol{\eta})$ | Restoring matrix |

*Process and control states and variables*

| | |
|---|---|
| $\boldsymbol{\eta}$ | Generalized position, low-frequency vessel motion |
| $\boldsymbol{\nu}$ | Generalized velocity |
| $\boldsymbol{\nu}_r$ | Generalized relative velocity |
| $\boldsymbol{W\xi}$ | Wave frequency vessel motion |
| $\mathbf{b}$ | Bias state including slowly varying and unmodeled dynamics |
| $\mathbf{v}$ | Measurement noise vector |
| $\mathbf{y}$ | Measurement vector containing low frequency and wave frequency vessel motion, and noise |
| $\mathbf{u}$ | Control input |
| $\boldsymbol{\eta}^*$ | Generalized desired position |
| $\hat{\boldsymbol{s}}$ | Estimate of $\mathbf{s}$, where $\mathbf{s}$ is a state or variable, e.g. $\hat{\boldsymbol{\eta}}$ is the position estimate, $\hat{\boldsymbol{\nu}}$ is the velocity estimate, etc. |

*Hybrid states and variables*

| | |
|---|---|
| $\mathbf{x}$ | Hybrid state containing continuous and discrete states |
| $\tau$ | Timer variable triggering switching |
| $\mathcal{A}$ | The set of values $\mathbf{x}$ takes when it is controlled to the reference |

*Environmental variables*

| | |
|---|---|
| $H_s$ | Significant wave height |
| $\omega_p$ | Peak wave frequency |

# Contents

# Chapter 1

# Introduction

The first oil-find on the Norwegian continental shelf was made in 1969 at 70 meter water depth at the Ekofisk field. This was the start of the Norwegian oil adventure. More than 40 years later there is still high activity on the continental shelf, with Norway as the largest oil producer in Europe, and the second largest natural gas exporter world wide (US Energy Information Administration). Exploration and production activities have shifted from easily accessible waters into more remote and extreme environments, and experience and technology have developed accordingly. For instance the number of vessels with dynamic positioning (DP) capabilities has increased significantly, and are today essential in fields like offshore oil and gas, aquaculture, renewable energy, as well as in emerging fields like offshore mining. In order to maintain continuous and safe marine operations in increasingly challenging environments, the demand of dynamic positioning (DP) classed marine vessels has grown, leading to soaring day rates.

## 1.1 Motivation

Today the main focus is on extending the operational window for vessels so that waiting time for a sufficient weather window to conduct an operation is decreased. The success of a marine operation is highly dependent on statistical weather date from the region, local weather forecast as well as the weather time history for the past hours in the surrounding area. The first phase of a marine operation is planning all details of the operation so it can be completed safely within the weather window available. A maximum allowable response for the vessel is set based on the type of operation, water depth and vicinity to other structures, and a threshold wave height and frequency is calculated. These are compared with historical weather statistics from the operational area, and a time domain simulation of a complete environmental description is completed.

Take for example a lifting operation through a moonpool. According to DNV's recommended practices for marine operations DNV (2014), with incident waves

with mean zero-crossing period $T_z = 8$ seconds, the maximum allowable significant wave height ($H_s$) is 2.5 meters for this type of operation. If for instance this operation is to be conducted in the northern North Atlantic, statistics from this region indicate that around 50 % of the time the significant wave height is lower than this (Price & Bishop, 1974), and the operation may be conducted. The local weather forecast and the operation time further limits the weather window, especially in the transition to winter when rougher sea states occur. Large marine operations may have a duration of several weeks to months, driving the operation costs up as vessels wait for a sufficiently large weather window to complete the operation.

## 1.2 Previous Work

In normal operational conditions the first order wave induced motions, usually with dominating wave periods in the order of 5-10 seconds, of the vessel are filtered through a wave-filter before entering the control law. This means that the vessel is supposed to follow the waves back and forth around the desired setpoint, and not compensate for wave frequency motions using the thrusters. In extreme operational conditions the wavelength and periods become longer, and the horizontal motions of dynamically positioned vessels become correspondingly larger. Sørensen, Strand, Nyberg & Simrad (2002) proposes a DP system structure for floating structures in extreme seas where the wave filtering in the observer has been eliminated so wave compensation is achieved. The DP control algorithms for normal and extreme conditions can beneficially have different structures, motivating the combination of several systems into one. Using existing hybrid frameworks is a way of doing this.

A hybrid system combines dynamics that change at different time scales, for example continuously and instantaneously, into one system. Two different modeling frameworks are introduced; the *flows and jumps* framework proposed by Goebel, Sanfelice & Teel (2012), and the *switched system and supervisor* framework described in Hespanha (2002), Hespanha & Morse (2002), Hespanha, Liberzon & Morse (2003). The first framework is used in this thesis, and the other framework has earlier been applied to DP.

The hybrid systems framework proposed by Goebel et al. (2012) is a general formulation of a system where the state can evolve both by *flowing* by a differential relation in continuous-time and *jumping* by a difference relation in discrete time. The advantage of this model formulation is that it can be applied to many different types of hybrid systems, for instance systems with logical variables, impacts or measurement sampling with different sample times. When a hybrid system satisfies certain regularity properties, then stability and robustness results from Goebel et al. (2012) can be applied to analyze the system. The stability results are based

on known results from nonlinear system theory, see Khalil (2002) for more on nonlinear systems.

Hespanha (2002), Hespanha & Morse (2002) and Hespanha et al. (2003) proposes a hybrid system structure where the process (switched system) is monitored by a *supervisor*. The supervisor contains several models of the system, or other decision logic, so it can be determined which candidate controller from the bank is likely to yield the best vessel performance. A switching algorithm is implemented which ensures smooth switching and prevents *chattering*; the rapid switching back and forth between controllers. Chattering may destabilize the hybrid system.

The hybrid control concept outlined in Hespanha (2002), Hespanha & Morse (2002) and Hespanha et al. (2003) has been explored for marine applications in Nguyen, Sørensen & Quek (2007, 2008). Nguyen et al. (2007) proposes a hybrid controller for DP for environmental variations from calm to extreme seas. The major findings were that the hybrid controller performs better than a single controller in sea states that vary from calm to extreme. Nguyen et al. (2008) extended the same concepts to include models where the vessel is in maneuvering and transit modes in addition to stationkeeping.

Apart from the control algorithm, another important component of a DP system is the observer. The main task of an observer is to estimate the vessel motion based on noisy measurements. It takes in measurements of some vessel states with different sensors, which introduce noise and bias on the signal, and use this information to generate estimates of all unmeasured states. Sensors are costly, so having an observer is an inexpensive way of obtaining all necessary information about the vessel motion. The vessel oscillates with the first order incident waves. Most observers include a wave filter, which takes away the wave frequency vessel motion in normal operational conditions in order to reduce wear and tear on the machinery and thrusters. The observer should also estimate the steady state deviation of the vessel from the desired setpoint, also called the bias. It is a measure of the mean forces acting on the vessel from current, mean wind, slowly varying waves, and unmodeled dynamics like damping. In the case of measurement signal loss, the observer should also be able to predict the vessel position in dead reckoning mode.

Two main observer types are used for marine applications, the model-based like the extended Kalman filter (Tannuri & Morishita, 2006), (Hassani, Sørensen & Pascoal, 2013), or a nonlinear passive observer (NPO) (Fossen & Strand, 1999), and the sensor-based approach (Vik & Fossen, 2001),(Farrell, Givargis & Barth, 2000). The model-based observer uses a simplified mathematical model of the vessel and noisy measurements to estimate and predict states. The sensor-based approach is based on the integration of acceleration measurements from the inertial reference units and comparing this with GNSS (global navigation and sensor system) position measurements.

One weakness of model-based observers is the bias estimation in the case where

the mean environmental forces acting on the vessel changes quickly. In order to have accurate bias estimates the estimator dynamics need to be slow, hence a trade-off exists for estimation accuracy and speed. Because the bias component may be large, inaccurate bias estimation may cause drift-off of the vessel and in turn lead to disconnect and operation stop. A downside to the sensor-based observer is that it cannot be used of state prediction during signal loss because it requires measurements to supply estimates. It therefore needs to be paired with an observer which works during signal failure in order to satisfy redundancy requirements (DNV, 2013).

## 1.3 Main Contributions

The main contributions of this thesis is the application of the hybrid framework proposed by Goebel et al. (2012) to high-level control of marine vessels. The appended papers include two different applications, and the individual contributions are summarized below. Both papers are submitted to conferences for publication.

**Paper 1** *To be published at the ASME 2014 33$^{rd}$ International Conference on Ocean, Offshore and Arctic Engineering, OMAE 2014.* A hybrid DP controller for a vessel in a varying sea state is designed, and global asymptotic stability is established. Simulations in a sea state varying from calm to extreme are conducted with the hybrid controller containing four candidate controllers, and a single controller with adaptive wave filtering for comparison. The single controller becomes unstable in extreme seas whereas the hybrid controller shows good performance. Jumps between candidate controllers is based on spectral analysis of the vessel wave frequency motions.

**Paper 2** *Submitted to the 2014 IEEE Multi-conference on Systems and Control.* A simplified sensor-based hybrid observer concept is investigated for noise robust position estimation. The concept assumes that acceleration measurements are readily available, and can be integrated to obtain position estimates. Position measurements are taken occasionally, and at these instances the position estimate is updated. Major contributions of this paper include the design, stability analysis and simulation of two one degree of freedom sensor-based hybrid observers which rely on acceleration, velocity and position measurements.

## 1.4 Organization of the Thesis

This thesis is edited a collection of papers with a resume in front. The resume aims to improve readability of the papers by introducing background concepts more thoroughly and discussing the simulators giving the results presented.

Chapter 2 discusses the theory used in the papers more thoroughly. Topics covered include a short introduction to DP on a system level, mathematical modeling of marine vessels and frameworks describing hybrid dynamical systems.

In both papers simulation results for the controller and observers are presented. Chapter 3 describes the simulation models, discusses the simulation setup and the validation process of the simulators.

Chpater 4 concludes the thesis, summing up the major findings from the papers and suggesting further work.

Paper 1 is called *Increasing the Operation Window for Dynamic Positioned Vessels Using the Concept of Hybrid Control*, and addresses the design and stability analysis of a hybrid DP controller using the framework provided by Goebel et al. (2012). The performance of the hybrid controller is compared to a single controller with adaptive wave filtering for a vessel in a sea state changing from calm to extreme.

Paper 2 is called *Sensor-Based Hybrid Observer for Dynamically Positioned Vessels*, and covers a sensor-based observer concept which uses noisy acceleration, velocity and position measurements of different fidelity to calculate position estimates. The design and stability analysis is done using the hybrid framework by Goebel et al. (2012), and the system is simulated in one degree of freedom.

The Bibliography after Chapter 4 contains all references in the thesis i.e. including the references in Chapter 1 - 4 as well as those found in the appended papers.

# Chapter 2

# Background and Mathematical Modeling

This chapter discusses the background for this thesis further. The topics covered include an introduction to dynamic positioning, marine vessel modeling, and hybrid system modeling.

## 2.1 Introduction to Dynamic Positioning

A vessel in dynamic positioning (DP) uses the thrusters as the sole means of keeping position in wind, waves and current. A DP system can be defined as *the complete installation necessary for dynamically positioning a vessel comprised of the power system, thruster system, and DP control system* DNV (2013). The DP control system consists of computers including hardware and software, sensor system, displays and operator panels, positioning reference system, and the associated cabling. This thesis considers parts of the software within the DP control system, namely the *motion control system* and *observer*, which in literature is referred to as *high-level control*. Other aspects are not investigated.

The DP software consists of three independent blocks *guidance*, *navigation* and *control* (GNC) which have different tasks, see Figure 2.1. The guidance system computes continuous desired position, velocity and acceleration for the vessel. It receives waypoints based on weather data and operator inputs which describes the vessel's desired position at different times. It also uses estimates of the vessel's position, velocity and acceleration obtained by an observer to generate feasible desired references.

The navigation system is composed of a positioning system in combination with motions sensors like accelerometers and gyros, and an observer. Different types of positioning systems exist like for instance global navigation satellite system (GNSS), high precision acoustic positioning systems (HiPAP), and laser-based

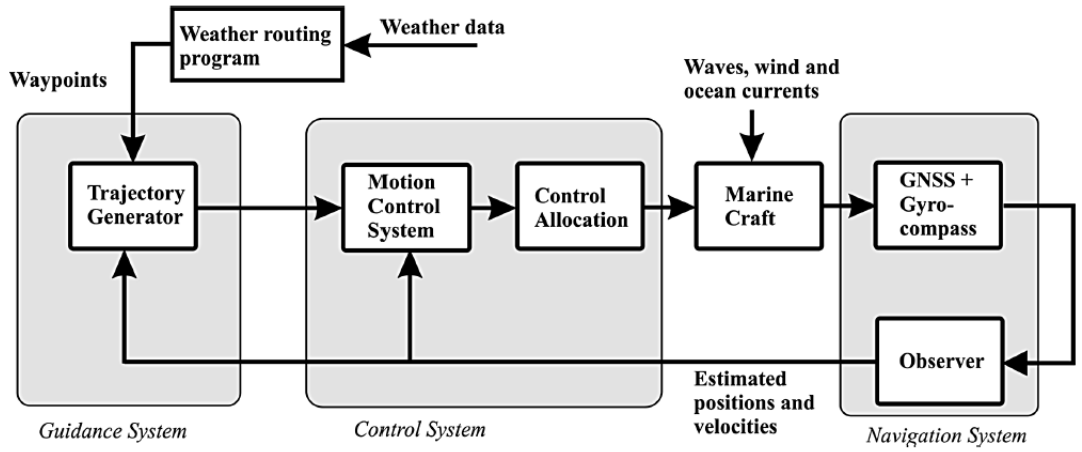


FIGURE 2.1: GNC flow map (Fossen, 2011).

positioning systems. Measurements of the vessel's motion are taken at different sampling rates, and are noisy and biased due to imperfect sensors. Sensors are expensive, so in stead of measuring all states that are required, some states are reconstructed from those that are measured by an observer. For example, by measuring the surge position and acceleration, an estimate of the surge velocity can be calculated. A system where the unmeasured states can be estimated from the measurements is said to be *observable*, which is a key observer property. In addition, the observer filters out the first order (wave frequency) vessel motions, and in the case of signal loss the states are predicted (dead reckoning). Observers are described more detailed in Section 2.3.

The control system takes in the desired and estimated position, velocity and acceleration, and calculates the required control forces in order to satisfy the *control objective*. Some examples of control objectives are setpoint regulation, trajectory tracking, path following and maneuvering. For DP, the control objective is to keep a fixed or slowly moving desired position and heading. The control objective depends on the operation taking place; lifting in air or water, mining or drilling at different water depths, or operations in the vicinity of other vessels.

The motion control system, later referred to as the controller, calculates control forces in the horizontal plane (surge, sway and yaw), based on the difference between the vessel's desired and estimated states. The control forces are distributed to each individual thruster through the control allocation, in order to obtain the correct thrust magnitude and direction. Section 2.4 discusses the control system further.

In the appended papers the focus is on the controller and observer. See Fossen (2011) for details on GNC systems.

## 2.2 Marine Vessel Modeling

This section introduces two models of different fidelities used when modeling a marine vessel; the process plant model and the control plant model.

### 2.2.1 Process Plant Model

The process plant model (PPM) is a high fidelity model which accurately describes the real vessel behavior. It is used in simulators for controller testing and verification, and includes process disturbances, sensor outputs and control inputs (Sørensen, 2011). The PPM is a six degree of freedom (6DOF) nonlinear low-frequency vessel model given by:

$$\mathbf{M}\dot{\boldsymbol{\nu}} + \mathbf{C}_{RB}(\boldsymbol{\nu})\boldsymbol{\nu} + \mathbf{C}_A(\boldsymbol{\nu}_r)\boldsymbol{\nu}_r + \mathbf{D}(\kappa, \boldsymbol{\nu}_r) + \mathbf{G}(\boldsymbol{\eta}) = \boldsymbol{\tau}_{env} + \boldsymbol{\tau}_{moor} + \boldsymbol{\tau}_{thr}, \quad (2.1)$$

where $\mathbf{M}$ is the inertia matrix including added mass, $\dot{\boldsymbol{\nu}}$ is the vessel acceleration, $\mathbf{C}_{RB}$ and $\mathbf{C}_A$ are the rigid body and added mass Coriolis matrices, $\boldsymbol{\nu}$ and $\boldsymbol{\nu}_r$ are the generalized velocity and relative velocity, $\mathbf{D} = \mathbf{D}_L + \mathbf{d}_{NL}$ is the damping matrix consisting of a linear and nonlinear term, $\mathbf{G}$ is the restoring matrix, $\boldsymbol{\eta}$ is the generalized position, and $\boldsymbol{\tau}_{env}, \boldsymbol{\tau}_{moor}$, and $\boldsymbol{\tau}_{thr}$ are the external forces acting on the ship from the environment, mooring and thrusters[1]. See Sørensen (2013) for more details on the matrices.

### 2.2.2 Control Plant Model

The control plant model (CPM) is a simplified vessel model including only the main physics. It is often included in model-based observers and controllers, and therefore needs to be computationally efficient. The CPM contains a simplified low frequency vessel model based on (2.1), a wave frequency vessel model, a bias model for slowly varying forces, and a coordinate transformation. For distinct vessel types, environmental conditions, and operations (control objectives), different physical effects matter, and hence the CPM takes various forms. The CPM for a non-moored ship-shaped surface vessel in normal environmental conditions is discussed first. Then the CPM for the same vessel type in extreme environmental conditions is introduced.

Firstly the PPM (2.1) is simplified for a surface vessel in DP in normal operational conditions. The vessel motions that may be controlled by the thrusters occur mostly in the horizontal plane, so heave, roll and pitch motions are neglected. By model reduction, this leaves the 3DOFs surge, sway and yaw $\boldsymbol{\eta} = [x, y, \psi]^T$, $\boldsymbol{\nu} = [u, v, r]^T$. In DP, the velocities $\boldsymbol{\nu}$ and $\boldsymbol{\nu}_r$ are small, so the physical effects

[1] $\boldsymbol{\tau}_{thr}$ is the actual thrust acting on the vessel. It is the output from the control allocation block, see Figure 2.1, minus thruster losses due to thruster-hull and thruster-thruster interaction, cavitation, ventilation, etc. Sørensen (2013) has more details.

of $\mathbf{C}_{RB}(\boldsymbol{\nu})\boldsymbol{\nu}$ and $\mathbf{C}_A(\boldsymbol{\nu}_r)\boldsymbol{\nu}_r$ can be assumed negligible. The same applies to the nonlinear damping term $\mathbf{d}_{NL}$. $\mathbf{G}(\boldsymbol{\eta})$ can be neglected in surge sway and yaw, as there is no restoring in these DOFs for a vessel that is not moored.

The acceleration and velocity measurements are in a body-fixed reference frame, and the position measurement and desired position are in a North-East-Down (NED) reference frame. The body-fixed frame rolls, pitches, and yaws, as well as moves translatory with the vessel motion. This introduces Coriolis terms relating the rotations of the body-frame to the NED frame. The NED frame creates a local tangent-plane at the Earth's surface close to where the vessel operates. It is assumed inertial for local marine vessel navigation purposes. A transformation is required in order to compare measurements, estimates, and references. The transformation of velocity in the body-fixed reference frame to the NED-frame is according to Fossen (2011) $\boldsymbol{\nu}^n = \boldsymbol{R}(\boldsymbol{\Theta})\boldsymbol{\nu}^b$, where $\boldsymbol{\Theta}$ are the rotations roll, pitch and yaw, and $\boldsymbol{R}(\boldsymbol{\Theta})$ is the 6DOF rotation matrix.

Applying the simplifications, adding a bias and wave-frequency model, and transforming the positions of (2.1) to the NED-frame yields the following CPM:

$$\dot{\boldsymbol{\xi}} = \mathbf{A}_\omega \boldsymbol{\xi} + \mathbf{E}_\omega \mathbf{w}_\omega, \tag{2.2a}$$
$$\dot{\boldsymbol{\eta}} = \mathbf{R}(\psi)\boldsymbol{\nu}, \tag{2.2b}$$
$$\dot{\boldsymbol{b}} = \mathbf{T}_b^{-1}\mathbf{b}(t) + \mathbf{E}_b \mathbf{w}_b, \tag{2.2c}$$
$$\mathbf{M}\dot{\boldsymbol{\nu}} = -\mathbf{D}\boldsymbol{\nu} + \boldsymbol{R}^T(\psi)\mathbf{b}(t) + \boldsymbol{u}, \tag{2.2d}$$
$$\mathbf{y} = \boldsymbol{\eta} + \mathbf{C}_\omega \boldsymbol{\xi} + \mathbf{v}. \tag{2.2e}$$

(2.2a) is the wave frequency model representing the first order wave response of the vessel. It is modeled as a damped oscillator driven by white noise $\mathbf{E}_\omega \mathbf{w}_\omega$. $\mathbf{A}_\omega$ is a matrix containing the peak wave frequency $\omega_p$ and a damping ratio $\lambda$ chosen according to the sea state and operating area (Fossen, 2011). In the North Sea, the sea state is often described using the JONSWAP (Joint North Sea Wave Project) wave spectrum, which is a spectrum for wind-generated and developing seas. The wave frequency model is used in model-based observers to eliminate the wave frequency vessel motion from the measurement to produce a low frequency estimate. In this way the vessel does not compensate for the oscillatory first order wave motion, thus reducing power consumption and wear and tear on the machinery. A wave filter using the an estimate of the actual frequency of the waves is called an adaptive wave filter Sørensen (2013).

(2.2b) is the 3DOF kinematics transforming velocity from the body-fixed frame to the NED-frame, where

$$\mathbf{R}(\psi) = \begin{bmatrix} cos(\psi) & -sin(\psi) & 0 \\ sin(\psi) & cos(\psi) & 0 \\ 0 & 0 & 1 \end{bmatrix} \tag{2.3}$$

is the rotation matrix, $\boldsymbol{\nu}$ is the body-fixed velocity and $\dot{\boldsymbol{\eta}}$ is the NED velocity. Integrating gives NED position $\boldsymbol{\eta}$.

(2.2c) is the bias model which contains damping, unmodeled dynamics and slowly varying forces such as current and wave drift. It is here described by a Markov process where $\mathbf{T}_b^{-1}$ is a user-specified diagonal matrix with positive bias constants, and $\mathbf{w}_b$ is a vector of zero mean Gaussian distributed white noise. The bias $\mathbf{b}(t)$ is a measure of the mean forces acting on the vessel, and is estimated by a model-based observer, see Section 2.3 for details. It is important that the bias estimate corresponds with reality because it may be large, and estimating incorrectly may cause drift-off of the vessel, operation stop, and in the worst case a blow-out or other accident. The bias estimation has slow dynamics with time scale $\mathbf{T}_b$, and is therefore vulnerable to environmental changes that happens faster than this. There is a trade-off on how large $\mathbf{T}_b$ should be because a large value makes the bias estimates accurate, but slow.

(2.2d) is the simplified low-frequency vessel model based on (2.1) where only the linear term is kept in $\mathbf{D}$, and $\boldsymbol{u}$ is the control input to the control allocation. (2.2e) is the measurement equation imitating the output from the sensors, including low-frequency motions $\boldsymbol{\eta}$, wave-frequency motions $\mathbf{C}_\omega\boldsymbol{\xi}$ and measurement noise $\mathbf{v}$. There are twelve states in the 3DOF CPM; $[\boldsymbol{\xi}^T, \boldsymbol{\eta}^T, \mathbf{b}^T, \boldsymbol{\nu}^T]^T$. For more details on CPM modeling, see Sørensen (2013).

### Control Plant Model for Extreme Sea States

As briefly mentioned, the CPM for extreme sea states is slightly different from the one previously described. The preliminaries are discussed before the CPM for extreme sea states is presented.

Price & Bishop (1974) divided the environmental condition into different sea states according to the measured wave height and frequency, see Table 2.1.The probability of occurrence of the different sea states in the northern North Atlantic, including the North Sea, is also given, where sea states 3, 4, and 5 occur the most often. This is also dependent on the season, as rougher sea states occur more often in the winter time. In this thesis, the sea states *very high* and up are referred to as extreme sea states.

A sea state can be described mathematically by a wave spectrum, see Figure 2.2 for an example, with the significant wave height $H_s$ and a characteristic wave frequency, here the peak wave frequency $\omega_p$ is used. $S(\omega)$ represents the energy in the sea state at different frequencies $\omega$, i.e. waves with frequency near $\omega_p$, where $S$ is maximum, occur more often. The sea surface elevation for a sea state can be generated by summing up different wave components with frequency and energy distributions as given in the wave spectrum. In the North Sea a JONSWAP spectrum is often used to describe a sea state. Double peaked wave spectra also exist for describing swell-dominated seas.

TABLE 2.1: Definition of the sea state codes as given by Price & Bishop (1974). The percentage probability for sea states 0-2 is summarized.

| Sea State Code | Description of sea | Significant wave height ($H_s$) [m] | Peak wave frequency ($\omega_p$) [rad/sec] | % probability Northern North Atlantic |
|---|---|---|---|---|
| 0 | Calm (glassy) | 0 | 1.29 | |
| 1 | Calm (rippled) | 0-0.1 | 1.29-1.11 | 6.0616 |
| 2 | Smooth (wavelets) | 0.1-0.5 | 1.11-0.93 | |
| 3 | Slight | 0.5-1.25 | 0.93-0.79 | 21.5683 |
| 4 | Moderate | 1.25-2.5 | 0.79-0.68 | 40.9915 |
| 5 | Rough | 2.5-4.0 | 0.68-0.60 | 21.2383 |
| 6 | Very rough | 4.0-6.0 | 0.60-0.53 | 7.0101 |
| 7 | High | 6.0-9.0 | 0.53-0.46 | 2.6931 |
| 8 | Very high | 9.0-14.0 | 0.46-0.39 | 0.4346 |
| 9 | Phenomenal | Over 14 | Less than 0.39 | 0.0035 |

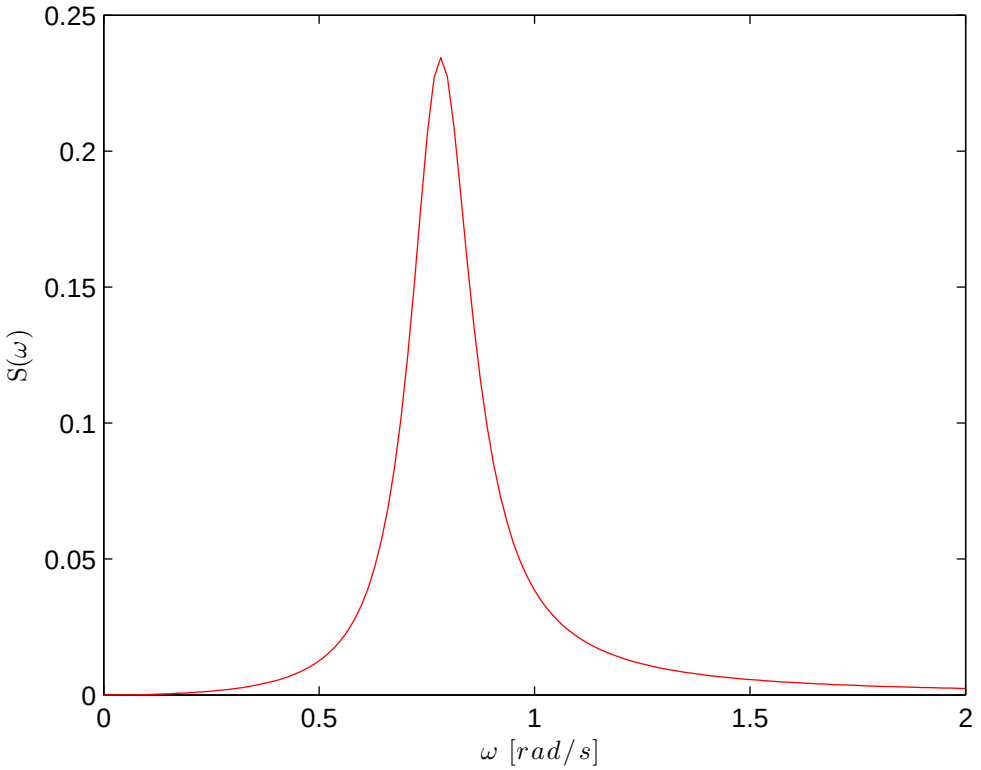


FIGURE 2.2: A conceptual sketch of a wave spectrum $S(\omega)$ for first order waves.

As the sea state increases, see Table 2.1, the significant wave height $H_s$ increases, and the peak wave frequency $\omega_p$ decreases. Increasing the significant wave height leads to larger relative motion between the vessel and the sea surface, i.e. larger motion in the vertical direction. The previous assumption of small heave, roll and pitch motions are in this case questionable. However for a ship-shaped

vessel small compensation[2], if any, may be achieved in these DOFs by use of thrusters. Ventilation and cavitation on the thrusters is an increasing problem for higher waves, leading to more thruster loss, which is difficult to account for. In addition the vessel-fluid interaction includes more nonlinearities especially altering the damping term $\mathbf{D}\boldsymbol{\nu}$. However, the main concern for DP in an increasing sea state is the decreasing frequency of the waves, as physics related to the increasing wave height are difficult to control.

Decreasing wave frequency leads to two main problems related to the horizontal motion of the vessel; the amplitude and frequency of the response. A wave with small $\omega_p$ will have a long wavelength, and if the vessel is allowed to move with the wave, it will have a corresponding large motion amplitude. Depending on the type of operation taking place, there is a set limit for how far the vessel is allowed to move from the desired setpoint or path. In these situations the vessel needs to compensate for the wave motion in order to continue the operation.

The second problem relates to the low frequency of motion the incident waves induce. $\omega_p$ and hence the wave frequency vessel motion approaches the low-frequency regime where ocean current, wave drift forces and mean wind forces are found. A wave filter, recall (2.2a), using $\omega_p$ may in this case filter out motions related to second order difference and mean waves, current and wind, thus leading to vital information loss. The estimated states will then be incorrect, leading to instability of the closed-loop vessel, observer, and controller system.

Compensation for wave frequency motion is achieved by excluding the wave frequency model from the control plant model (2.2a). This is investigated by Sørensen et al. (2002), giving the CPM for extreme sea states and for swell-dominated seas,

$$\dot{\boldsymbol{\eta}} = \mathbf{R}(\psi)\boldsymbol{\nu}, \tag{2.4a}$$

$$\dot{\boldsymbol{b}} = \mathbf{E}_b \mathbf{w}_b, \tag{2.4b}$$

$$\mathbf{M}\dot{\boldsymbol{\nu}} = -\mathbf{D}\boldsymbol{\nu} + \boldsymbol{R}^{\boldsymbol{T}}(\psi)\mathbf{b}(t) + \boldsymbol{u}, \tag{2.4c}$$

$$\mathbf{y} = \boldsymbol{\eta} + \mathbf{v}. \tag{2.4d}$$

The difference from (2.2) is that the wave frequency model is excluded, and the bias model is changed to a Wiener process.

In addition to waves described in Table 2.1, the environment also includes wind and current. Wind loads can be modeled as a mean wind velocity and an oscillatory component which acts on the vessel's superstructure. It is usually canceled by a feedforward term in the controller from the wind sensor. Current loads are included

[2]Roll and pitch damping is applied for semisubmersible platforms. Due to the small water plane area of these vessels, the natural frequencies of oscillation in roll and pitch are about the same as the incident waves in normal sea states. Roll and pitch damping is investigated by Sørensen & Strand (2000).

in the bias dynamics (2.2c) or (2.4b). For more details on marine environment modeling, see Faltinsen & Loken (1979), and Faltinsen (1993).

## 2.3 Observer

There are two main types of observers which are widely used in marine vessel navigation systems; model-based and sensor-based observers. Both observer types use noisy measurements from the sensors to reconstruct unmeasured states, filter out wave frequency vessel motions and estimate bias.

### 2.3.1 Model-based Observer

A model-based observer is an estimator based on the CPM (2.2) or (2.4), for example an extended Kalman filter (Tannuri & Morishita, 2006), (Hassani et al., 2013), or a nonlinear passive observer (NPO) (Fossen & Strand, 1999). The NPO is discussed further below as it is applied in the first appended paper. The advantage of a NPO over the extended Kalman filter is that the yaw dynamics does not need to be linearized, hence the vessel and observer has a global stability result. In addition, the tuning is easier than for instance an extended Kalman filter because there are less states to tune, see (Fossen, 2011) for details. The NPO algorithm is a copy of the CPM (2.2) including a correction term $\mathbf{K}_i\tilde{\boldsymbol{y}}$.

$$\dot{\hat{\boldsymbol{\xi}}} = \mathbf{A}_\omega\hat{\boldsymbol{\xi}} + \mathbf{K}_1(\omega_p)\tilde{\boldsymbol{y}}, \tag{2.5a}$$

$$\dot{\hat{\boldsymbol{\eta}}} = \mathbf{R}(\psi)\hat{\boldsymbol{\nu}} + \mathbf{K}_2\tilde{\boldsymbol{y}}, \tag{2.5b}$$

$$\dot{\hat{\boldsymbol{b}}} = \mathbf{T}_b^{-1}\hat{\mathbf{b}} + \mathbf{K}_3\tilde{\boldsymbol{y}}, \tag{2.5c}$$

$$\mathbf{M}\dot{\hat{\boldsymbol{\nu}}} = -\mathbf{D}\hat{\boldsymbol{\nu}} + \boldsymbol{R}^T(\psi)\hat{\mathbf{b}} + \boldsymbol{u} + \boldsymbol{R}^T(\psi)\mathbf{K}_4\tilde{\boldsymbol{y}}, \tag{2.5d}$$

$$\hat{\mathbf{y}} = \hat{\boldsymbol{\eta}} + \mathbf{C}_\omega\hat{\boldsymbol{\xi}}. \tag{2.5e}$$

$\tilde{\boldsymbol{y}} = \boldsymbol{y} - \hat{\boldsymbol{y}}$ is the estimation error and $\mathbf{K}_i, i = 1, 2, 3, 4$ are observer gain matrices, $\mathbf{K}_1(\omega_p) \in \mathbb{R}^{6\times3}$, and $\mathbf{K}_2, \mathbf{K}_3, \mathbf{K}_4 \in \mathbb{R}^{3\times3}$. Tuning the gains according to Fossen (2011) yields the observer passive and globally exponentially stable. $\hat{\boldsymbol{\eta}}$ is the estimate of $\boldsymbol{\eta}$, $\hat{\boldsymbol{\nu}}$ is the estimate of $\boldsymbol{\nu}$, and so on. By setting $\mathbf{C}_\omega = \mathbf{0}$ the wave filtering is turned off.

The thicker line in Figure 2.3 shows a Bode plot of the NPO, where the logarithmic wave frequency is along the horizontal axis, and the amplification in Decibel and phase in Degrees is along the vertical axis. The environmental forces acting on the vessel are indicated in words, and the wave spectrum for first order waves with $\omega_p \approx 0.8$ inserted with a thinner line. Focusing on the top plot, to the right the low-pass filter takes away rapid varying disturbances like noise, and the notch (wave filter) provided by (2.5a) takes away most of the first order wave frequency vessel motion. Towards the left in the plot, the low-frequency forces are canceled

by integral action. In this figure, it is clear that for low $\omega_p$, the notch effect may take away mean wave drift forces and slowly varying forces in addition to the first order wave forces.

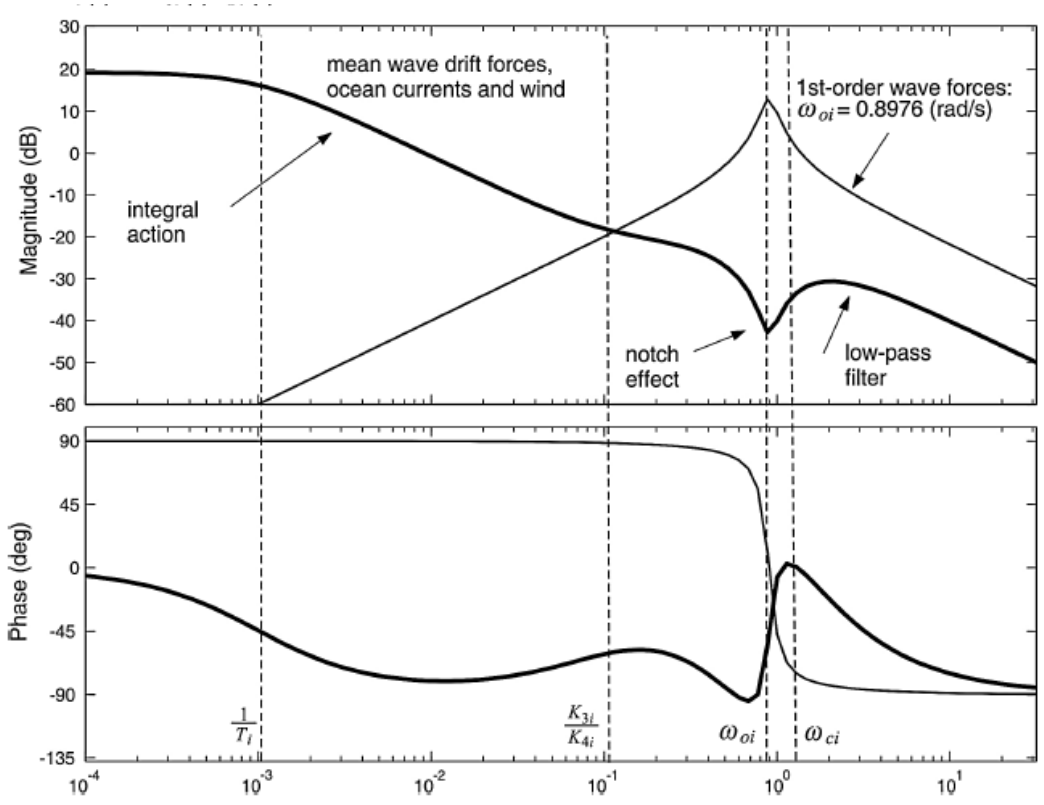


FIGURE 2.3: Nonlinear passive observer Bode plot (Fossen, 2011). $\log(\omega)$ is on the horizontal axis, and the amplification in Decibel and the phase in Degrees of the signal is on the vertical axis.

### 2.3.2 Sensor-based Observer

The sensor-based observer, or strap-down approach, uses only measurements to recreate states. Hua (2010) presents a method for estimating linear and angular velocity of accelerated vehicles by using linear and angular acceleration measurements. Based on this, Vik & Fossen (2001) and Farrell et al. (2000) propose an observer which integrates acceleration measurements twice to obtain position estimates, which are corrected with position measurements from for example GPS or HiPAP systems. It is found that accelerometer bias and drifting may cause large deviations in the position estimates due to the double integration.

In principle, a sensor-based observer may be used on any vessel and in any mode of operation since it is only based on measurements, whereas the model-based observer would need to be tuned for different vessels and applications. For the case of sudden bias changes, sensor-based observers generally have better performance than model-based observers due to the bias estimation problem, see

Section 2.2.2. However, in case of signal loss, the sensor-based observer cannot do dead reckoning, as it cannot predict an estimate without a measurement. Solutions to this problem include pairing the sensor-based observer with a model-based to satisfy the redundancy requirement (DNV, 2013).

The second appended paper looks at designing a sensor-based observer where the position, velocity and acceleration measurements are taken at different sampling rates, and which is robust to sensor noise.

## 2.4 Dynamic Positioning Controller

The DP controller takes in the desired and estimated position, velocity and acceleration, and calculates the thruster forces in surge, sway and yaw. There are different methods of doing this, reflected in the control algorithm in the DP software. The control algorithm is chosen based on the control objective, which is discussed in the first subsection. The second subsection is dedicated to the proportional, integral, derivative (PID) controller, which is widely used for DP and is applied in the first of the appended papers.

### 2.4.1 Control Objective

The control objective for a vessel in DP is to keep position with minimal standard deviations from the desired position while minimizing power consumption. This means that the error $\mathbf{e}$ between the generalized position $\boldsymbol{\eta}$ and the desired $\boldsymbol{\eta}^*$ should converge to zero as time increases

$$\lim_{t\to\infty} \mathbf{e} \to \mathbf{0} \tag{2.6}$$

subject to minimum energy consumption. $\boldsymbol{\eta}^*$ is the desired position $(x^*, y^*)$ and heading $\psi^*$ in the NED reference frame. $\psi^*$ is usually in the direction of the mean environmental loads. Keeping position with great accuracy and minimizing power consumption is an optimization problem where the cost function

$$\mathcal{J} = \int_{t=0}^{\infty} [\mathbf{z}\mathbf{Q}\mathbf{z}^T + \mathbf{u}\mathbf{R}\mathbf{u}^T]dt, \tag{2.7}$$

is sought minimized. $\mathbf{z}$ is a vector containing the vessel states, e.g. position $\boldsymbol{\eta}$, $\mathbf{u}$ is the control input, and $\mathbf{R}$ and $\mathbf{Q}$ are user-specified matrices. $\mathbf{R}$ and $\mathbf{Q}$ can then be tuned so that some states are punished more than others if they are large. This could be done with for example Linear Quadratic Gaussian (LQG) control design. In this thesis it is not investigated further, but this type of control design is especially important for the operational costs of the vessel. See Nocedal & Wright (2006) for more on numerical optimization. In stead, the minimum error part is satisfied by a PID control algorithm, and the minimum energy part is satisfied by

not compensating for small waves.

Figure 2.4 shows a conceptual sketch of the control objective. The origin of the coordinate system is placed in the desired position $\boldsymbol{\eta}^*$, and the control objective is to place the vessel-fixed point $CO$ at the origin, while keeping the bow against the mean environmental forces. In the figure, the environmental forces come from the same direction. In reality this may not be the case, for instance swell from a storm far away is not necessarily in the same direction as the local first order waves. Finding $\psi^*$ is then an optimization problem of finding the heading that minimizes the forces on the hull. As mentioned in Section 2.2.2, wave motion compensation should not be used unless the sea state is extreme.

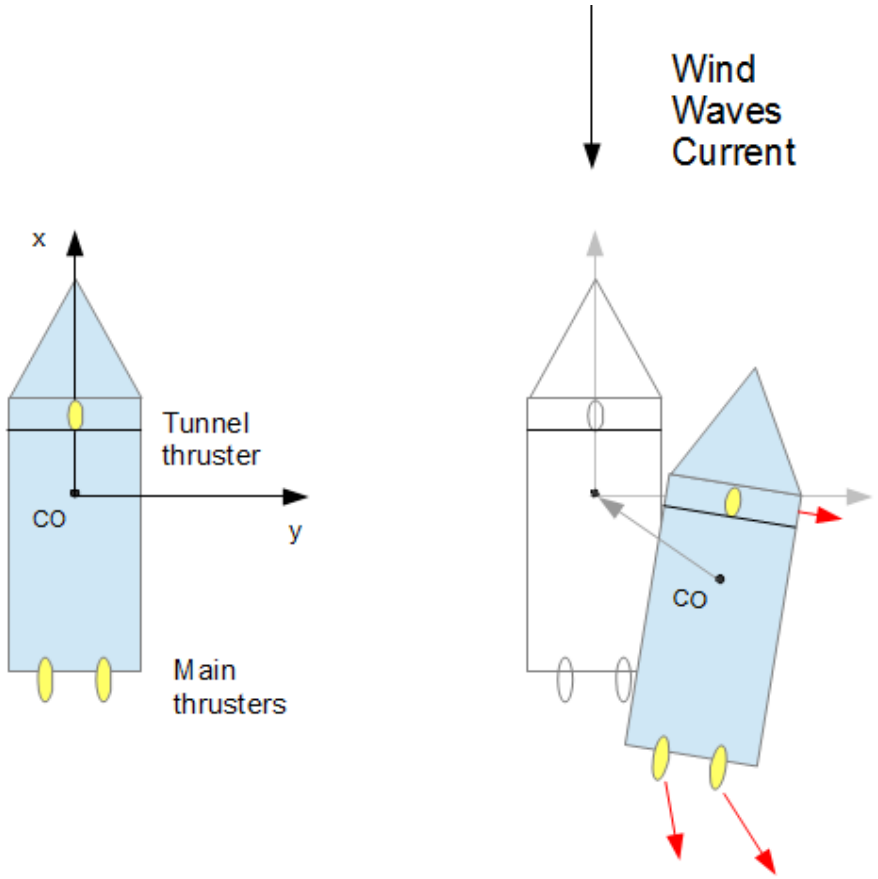


FIGURE 2.4: A conceptual sketch of the DP control objective.

### 2.4.2 Nonlinear PID Control Algorithm

For DP, the nonlinear PID control algorithm is widely used due to the intuitive design and tuning procedures. The algorithm has three terms, which control different aspects of the vessel motion. The proportional term acts on the position error from the desired position, decreasing in strength as the vessel approaches $\boldsymbol{\eta}^*$. The derivative term acts on the velocity of the vessel, controlling the speed

it moves with. When the vessel is close to the desired position the proportional term is small, and the vessel will usually not reach the desired position without an integral term. The integral term integrates the steady state position error over time, creating that extra control input necessary to reach $\boldsymbol{\eta}^*$. The controller uses estimates of the position and velocity in the control algorithm, which is:

$$\dot{\boldsymbol{\zeta}} = \hat{\boldsymbol{\eta}} - \boldsymbol{\eta}^*, \tag{2.8a}$$

$$\boldsymbol{u} = -\mathbf{R}^T(\psi)\boldsymbol{K}_p(\hat{\boldsymbol{\eta}} - \boldsymbol{\eta}^*) - \boldsymbol{K}_d\hat{\boldsymbol{\nu}} - \mathbf{R}^T(\psi)\boldsymbol{K}_i\boldsymbol{\zeta}, \tag{2.8b}$$

where $\boldsymbol{\zeta}$ is the integral state, $\hat{\boldsymbol{\eta}}$ is the position estimate, $\boldsymbol{\eta}^*$ is the desired position, $\mathbf{u}$ is the control input, $\hat{\boldsymbol{\nu}}$ is the velocity estimate, and $\mathbf{K}_j, j = p, d, i$ are gain matrices to the corresponding term. The transposed rotation matrix $\mathbf{R}^T(\psi)$ transforms the terms from the NED frame to the body frame, as the estimates and desired values are given in the NED frame, and the thrusters are bod-fixed.

Some other examples of control algorithms used for marine applications include energy minimizing algorithms, as briefly mentioned in the previous subsection, and model-based algorithms constructed using nonlinear control theory, see Fossen (2011) for an introduction to these topics.

## 2.5 Hybrid System Modeling

A dynamical system is usually classified as a continuous-time dynamical system, or a discrete-time dynamical system. However, many systems exhibit characteristics of both continuous and discrete time, and are referred to as *hybrid dynamical systems*, or simply hybrid systems. Branicky (1995) has examples of different types of hybrid systems. Several different frameworks are available to model such systems, and two are presented here. The first framework, which is applied in the appended papers, is a combination of continuous (*flow*) and discrete (*jump*) dynamics into one structure. The second framework has been applied before to a marine DP controller, and describes the hybrid system as a *switched system* and *supervisor*.

### 2.5.1 Flows and Jumps

A hybrid system, as modeled by Goebel et al. (2012) is a combination of a continuous-time system and a discrete-time system, where the state can evolve both by flowing in continuous-time and jumping in discrete time. A general mathematical model is,

$$\mathbf{x} \in C \quad \dot{\mathbf{x}} \in F(\mathbf{x}), \tag{2.9a}$$

$$\mathbf{x} \in D \quad \mathbf{x}^+ \in G(\mathbf{x}), \tag{2.9b}$$

where $\mathbf{x}$ is the hybrid state, $C$ is the *flow set*, $F$ is the *flow map*, $D$ is the *jump set*, and $G$ is the *jump map*. When the values of the hybrid state are in $C$, the

system will *flow* according to the differential relation $\dot{\mathbf{x}} \in F(\mathbf{x})$, and when $\mathbf{x}$ is in $D$, the state will *jump* according to the difference relation $\mathbf{x}^+ \in G(\mathbf{x})$. The $\mathbf{x}^+$ refers to the *next value of* $\boldsymbol{x}$ after a jump. Rapid successive jumping, also called *chattering*, is avoided when defining the flow and jump sets. The advantage of this model formulation is that it can be applied to many different types of hybrid systems, like systems with logic variables, mechanical systems with impacts, and computer sampled systems. A simple example of the modeling of a car is given below. For more motivational examples, see Goebel et al. (2012).

**Example: A car modeled as a hybrid system with flows and jumps**

When driving a stick-shift car, the driver has two main methods of controlling the car's speed; the gas pedal and breaks, and the gear. The gas pedal and breaks have relatively slow dynamics, and control the car speed in a nearly continuous manner. In comparison, the change of gear happens on a much smaller time scale, and may be regarded as an instantaneous event. As a simplified model, the speed $v$ of the car can be modeled in the flow map $F$, and the change of gear can be modeled in the jump map $G$.

The flow and jump sets determine when flows and jumps are allowed. At low speed, a low gear is preferable, and at higher speed a higher gear is preferable, so at an intermediate speed the gear should be changed. Assume that a car has five gears; $q = \{1, 2, 3, 4, 5\}$, where $q$ indicates the gear number. Then there are four intermediate speeds $\{v_{12}, v_{23}, v_{34}, v_{45}\}$ where a gear shift is triggered. Then we get:

$$
\begin{aligned}
&C := \mathbb{R} \times \{1, .., 5\} \\
&\quad \text{speed set} \times \text{gear set (flowing allowed)}, \\
&F := [f_v(q), 0]^T \\
&\quad \text{speed map, gear does not change by flowing}, \\
&D := \{v_{12}, v_{23}, v_{34}, v_{45}\} \times \{1, .., 5\} \\
&\quad \text{transitional speed} \times \text{gear set (jumping allowed)}, \\
&G := [v, g_q(v)]^T \\
&\quad v \text{ does not change, the next } q \text{ is chosen according to } v.
\end{aligned}
$$

Writing this in equation form gives:

$$
\begin{aligned}
v \in \mathbb{R} \quad \dot{v} &\in f_v(q), && \text{(2.10a)} \\
q \in \{1, .., 5\} \quad \dot{q} &= 0, && \text{(2.10b)} \\
v \in \{v_{12}, v_{23}, v_{34}, v_{45}\} \quad v^+ &= v, && \text{(2.10c)} \\
q \in \{1, .., 5\} \quad q^+ &\in g_q(v), && \text{(2.10d)}
\end{aligned}
$$

■

When a hybrid system is described using (2.9), and in addition is well-posed[3], then stability and robustness results from Goebel et al. (2012) can be applied to analyze the system properties. The stability results are based on results from nonlinear system theory, see Khalil (2002) for more on nonlinear systems.

### 2.5.2 Switched System and Supervisor

Supervisory switching is described extensively by Hespanha (2002), and this section is based on his tutorial. The principle can be summarized shortly in Figure 2.5, and is well suited for control applications. The bank of controllers contains $n$ candidate controllers suited for different conditions, the process is in this case a marine vessel, $w$ are environmental disturbances from waves, wind and current, $u$ is the control input to the thrusters, $y$ is the measurement, and $q$ is the switching signal. When the switching signal is constant, the chosen candidate controller and vessel is called the *switched system*, and contains the continuous dynamics. Compared with a controller with one candidate, a setup like this is beneficial in the case of largely varying disturbances, where the best suited candidate can control the vessel.

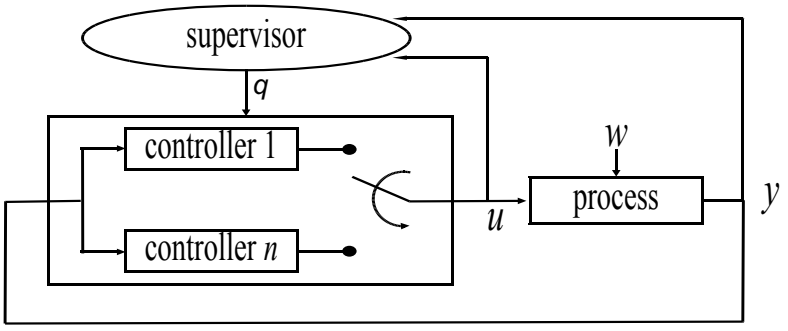


FIGURE 2.5: The supervisory switching principle (Hespanha, 2002).

The supervisor includes a *switching logic* with variable $q$, which is the discrete part of the hybrid system. It determines which controller to switch to using the process measurements $y$ and information about the controller performance. The switching logic should choose the controller which gives the smallest estimation error (or best performance) at all times. On the boundary between two operational regimes this might lead to chattering, the rapid switching back and forth between controllers. This should be avoided because it destabilizes the system. Switching in finite time can be ensured by for example dwell-time or hysteresis based switching logic. See Hespanha (2002), Hespanha & Morse (2002) and Hespanha et al. (2003) for details.

[3]Well-posedness is guaranteed by the data $(C, F, D, G)$ satisfying regularity properties; see (Goebel et al., 2012, Teorem 6.30). These regularity properties include $C$ and $D$ being closed; if $F$ and $G$ are functions defined on $C$ and $D$, respectively, then they should be continuous; here $F$ and $G$ are set-valued mappings, which are more general than functions. In that case, they should have closed graphs, be locally bounded, and should be nonempty on $C$ and $D$, respectively; moreover, the values $F(x)$ should be convex for each $x \in C$.

Modeling a hybrid controller with the different frameworks presented in this section makes the flow map analogous to the switched system and the jump map have similar tasks as the supervisor.

### 2.5.3 Hybrid Control in Marine Applications

The hybrid modeling framework based on *switched system and supervisor* has been explored for marine applications by Nguyen et al. (2007, 2008). Nguyen et al. (2007) proposes a hybrid controller for dynamic positioning in an environmental condition which changes from calm to extreme. Four sea states were defined according to significant wave height and corresponding frequency range in accordance with the Sea State Codes from Price & Bishop (1974), see Table 2.1. A bank with four different controllers and model sets were designed and tuned, one for each environmental condition. For calm and moderate seas the observers had wave frequency filtering and the controllers included proportional, integral and derivative gains (PID). For extreme seas the wave filtering was taken away and acceleration feedback was added to the PID controller. The fourth set designed for the transition from moderate to extreme seas was weighting of the moderate and extreme set to create a smooth transition. Switching was triggered by the predefined peak wave frequencies, which were estimated from the surge, sway and yaw vessel motions by spectral analysis.

The major findings were that the hybrid controller performs better than a single controller in sea states that vary from calm to extreme. It was also found that the PID controller with acceleration feedback reduced the standard deviation for both position and thrust in extreme seas compared with the PID controller without acceleration feedback.

Nguyen et al. (2008) extends the same concepts to include models where the vessel is in maneuvering and transit modes in addition to stationkeeping. Thus this paper introduces an integrated marine control system which allows smooth switching between controllers for specific operations subject to differing environmental conditions. The vessel operational conditions depend on operational mode[4], speed and the environment, which affect fundamental components of the control plant model. Each mode has a different control objective, speed changes affects the dynamic response of the vessel and thrusters, and the environment affects the frequency and intensity of disturbances. A case study keeping the environmental condition constant and varying the mode and speed yielded good results.

[4]Examples include DP, thruster-assisted position mooring, low-speed maneuvering, and transit.

# Chapter 3

# Simulation Setup and Validation

This chapter discusses the simulation setup and validation process for the hybrid DP controller and observers used to obtain the simulation results presented in the papers. In both cases Matlab/Simulink is used as the simulation tool.

## 3.1 Hybrid DP Controller Simulation

The hybrid DP controller was implemented into an existing Matlab/Simulink simulation model called MCSim, which is based on previous work done by Master and PhD candidates[1] at the Department of Marine Technology, NTNU. The model consists of three main parts; the environment module where waves, current and wind is generated, the marine vessel which consists of the vessel dynamics, and the GNC module which consists of guidance, navigation and control blocks, as described in Section 2.1. Figure 3.1 shows an overview of the simulation model. The three main components are briefly described below, where the contribution from this project is within the GNC module.

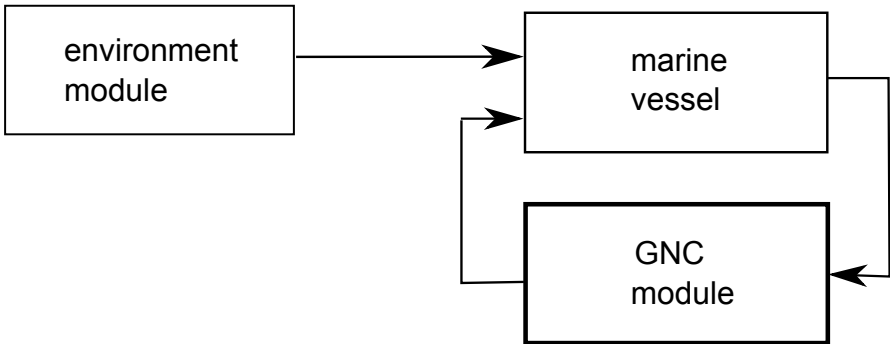


FIGURE 3.1: Block diagram showing the environmental module where waves, wind and current are generated, the marine vessel, and the GNC module containing guidance, navigation and controller blocks.

[1] Smogeli (2006), Nguyen et al. (2007, 2008), amongst others.

**Environmental Module**

The waves, wind and current are generated to simulate an irregular sea state which is slowly increasing over time. This is done by specifying the significant wave height and peak wave frequency pairs $(H_s, \omega_p)$ associated with the smallest and largest sea state. The intermediate sea states are calculated using steps between the minimum and maximum values, and the corresponding wave frequency $\omega$, direction $\psi_{wave}$, amplitude $\zeta_a = H_s/2$ and phase $\epsilon$ are calculated by using a JONSWAP wave spectrum. An irregular sea state is simulated by summing over $N$ wave components. The input to the marine vessel module is therefore a $(4 \times N)$ matrix containing $[\omega, \psi_{wave}, \zeta_a, \epsilon]$ for $N$ wave components.

The current is generated as a mean current velocity that increases slowly over time with mean incident direction towards the vessel's bow. The wind is generated using a NORSOK wind spectrum with increasing bow incident mean wind velocity as the simulation time increases.

In the simulation presented in the paper, the sea state is allowed to settle for 500 seconds, to ensure that the transient behavior has died out, before the sea state starts changing. The changes happen at intervals of 200 seconds, and the total simulation time is 11000 seconds. Because $\Delta\omega_p = 0.135$ and $\Delta H_s = 0.0148$ are small, the transient effects of the sea state change are assumed neglectible.

**Marine Vessel Module**

The marine vessel module is based on the PPM (2.1), and is a high fidelity model in 6DOFs including a low frequency and a wave frequency part. The vessel used in the simulations is a model of a 68 meter long platform supply vessel (PSV), see Figure 3.2 for thruster configuration and geometry.

The forces on the vessel from the environment and the thrusters are calculated using force response amplitude operators (RAO), see Fossen (2011) for calculation details. Based on the input $[\omega, \psi_{wave}, \zeta_a, \epsilon]$, the force in 6DOFs on the vessel can be calculated for each wave component and summed up to get the total force acting on the vessel. Using this approach, a time realization of the sea state is not required and much computational time is spared. The output from this module is the low frequency and wave frequency vessel motion, $\boldsymbol{\eta} + \mathbf{W}\boldsymbol{\xi}$.

**GNC Module**

Firstly the vessel motion is *measured* in the sensor system, and the simulated output is $\mathbf{y} = \boldsymbol{\eta} + \mathbf{W}\boldsymbol{\xi} + \mathbf{v}$, see Figure 2.1. The observer and motion controller are referred to as the hybrid DP controller, which is the contribution to the simulation model of the first appended paper.

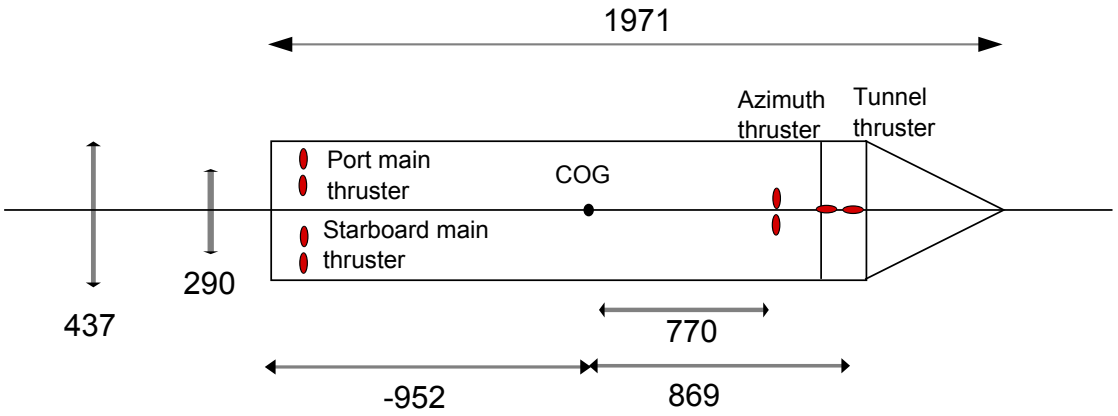


FIGURE 3.2: Cybership III thruster configuration, [mm].

The hybrid DP controller consists of four PID controllers and four NPOs, each designed for a specific sea state, see Table 3.1. An estimate of the sea state $q$ is obtained through spectral analysis of the wave frequency vessel response, and the corresponding controller and observer are chosen for output feedback.

| Sea State | $H_s$ [m] | $\omega_p$ [rad/s] | Controller | Observer | $q$ |
|---|---|---|---|---|---|
| 1 Calm | 1.25 | 0.79 | $PID_1$ | $NPO_1$ | 1 |
| 2 Moderate | 5.66 | 0.615 | $PID_2$ | $NPO_2$ | 2 |
| 3 High | 9.5 | 0.429 | $PID_3$ | $NPO_3$ | 3 |
| 4 Extreme | 14.0 | $\leq 0.279$ | $PID_4$ | $NPO_4$ | 4 |

TABLE 3.1: Sea state, controller, observer and switching signal $q$ overview. The values for $H_s$ and $\omega_p$ are given in full-scale, but are scaled down to model-scale in the simulations.

## Hybrid DP Controller Simulator Validation

The first phase of the simulator validation process was to check if the existing environment and vessel modules gave physically meaningful results. The vessel response was carefully observed first with no current and wind, and only one wave component, and finally with a changing sea state with wind and current. It was found that in order to obtain a physically meaningful vessel response, the sea state needed to change at a realistic time scale. A simulation time of 11500 seconds gave good results, but ideally the simulation could have a longer duration if more computational power was acquired.

The implementation of the hybrid controller was done in steps, focusing first on obtaining one independently working controller and observer. The other controllers and observers were implemented in a similar manner, and they were all tuned and tested in their design sea state. The final parts of the controller implemented were the spectral analysis and the switch allowing jumps.

## 3.2 Hybrid Observers Simulation

A block diagram showing the setup for the hybrid observer simulation model is shown in Figure 3.3. In stead of implementing a vessel model using the PPM as previously described in Section 3.1, the vessel position, velocity and acceleration $(\xi, v, a)$ are simulated using a third order reference model (Fossen, 2011). The reference model is usually applied in the guidance block to generate a smooth desired path for the vessel to follow. Assuming that a controller correctly and smoothly controls the vessel to the desired states, the reference model is a good simplification of the DP vessel dynamics. This is known as the *separation principle*, where the observer and the controller are designed independently of each other under the assumption that the observer dynamics are much faster than the process dynamics, see Fossen (2011) for details.

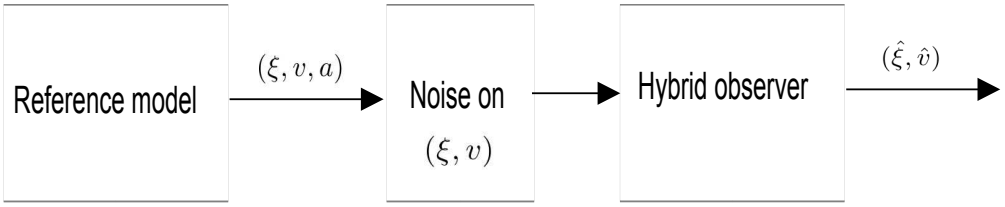


FIGURE 3.3: Block diagram of hybrid observer simulation model.

Zero mean Gaussian distributed noise is added to $(\xi, v)$, and this is assumed to be a good approximation for the vessel measurements. Both observers were implemented into Matlab/Simulink using the hybrid simulation toolbox described in Sanfelice, Copp & Ñañez (2013). The toolbox contains a structure for inserting the flow map, jump map, flow set and jump set directly.

### Hybrid Observer Simulator Validation

The third-order reference model was first implemented without noise, and the acceleration, velocity and position output were analysed to check that they were physically meaningful values like $a = \dot{v}$ and $v = \dot{\xi}$. The reference model was then tuned so it generated trajectories with similar time scales as the marine vessel module in MCSim, see the previous section. One hybrid observer was implemented and verified to estimate the exact position and velocity from the reference model, without the presence of noise. The second observer was implemented in a similar manner, and finally noise was added on $(\xi, v)$.

The results obtained with the simplified vessel model gives a good indication of the performance of the observers. However, the behavior of the observer in closed loop with an output feedback controller may be different than the results obtained here indicate. This is because when the observer estimates are used in the feedback law of the controller, the control forces and hence the vessel response is highly dependent on the quality of the estimates.

# Chapter 4

# Conclusion

In this thesis the performance of high-level hybrid DP control algorithms has been evaluated for a DP vessel in an extreme sea state. This chapter concludes the thesis summarizing the major results from the appended papers and including some suggestions for future work.

## 4.1 Concluding Remarks

In this thesis, the hybrid modeling framework proposed by Goebel et al. (2012) was applied to high-level DP control of a marine vessel. The framework was highly beneficial for this type of application, mainly due to the good mathematical modeling and stability tools.

In the first application, a hybrid DP controller was designed to cope with an environmental condition that changed from calm to extreme. The model was designed based on well-known marine CPMs, and included four observers and four controllers, each tuned for a specific sea state. An estimate of the sea state was used to decide which controller and observer to use, and this was based on spectral analysis of the surge, sway and yaw wave frequency vessel motions. The hybrid controller was shown globally asymptotically stable (GAS) by using set stability theory.

In the simulations conducted, the hybrid controller performed better than a single adaptive controller when the sea state changed from calm to extreme. As expected the single controller with adaptive wave filtering became unstable in extreme seas due to filtering of low frequency vessel motions. Using spectral analysis in surge, sway and yaw to estimate the sea state seemed to work well, and in the simulations instability due to jumps was not detected. The behavior of the sea state estimate acted as a hysteresis switching constraint on the system.

In the second application, a sensor-based hybrid observer concept using noisy position, velocity and acceleration measurements $(\xi, v, a)$ was designed for position

estimation. The observer was based on the integral relation between the measurements, namely $\dot{v} = a$ and $\dot{\xi} = v$, and used simple averaging of the observer's states ($N$ previous measurements) to eliminate the random noise component, and generate a position estimate. The acceleration measurement was assumed to be taken continuously, and the velocity and position measurements were assumed to be taken occasionally, with maximum update intervals of $T_{max}$ seconds. Thus the observer states used $a$ to *flow*, and *jumped* when new $(\xi, v)$ measurements were available. Two 1DOF observers were implemented and the difference was that observer 2 averaged two times; during jumps and during flows, and observer 1 only averaged during jumps. Uniform global asymptotic stability (UGAS) was proven.

The observers' performance was highly dependent on the number of states $N$ in the observer, the initializing of the observer states, and the maximum update time $T_{max}$. Observer 2 performs better for large $N$, and observer 1 performs better for small update intervals. Initializing the observers correctly was of increasing importance when $N$ increased. The effect of noise was reduced, and almost eliminated for certain combinations of parameters.

In conclusion, the hybrid systems framework (Goebel et al., 2012) used in this thesis is a powerful tool for marine control applications. Both the hybrid controller and observer concept show promising results regarding performance of a DP vessel in extreme sea states.

## 4.2 Suggestions for Further Work

There are a number of possible topics for further study, both on the simulation and theoretical side.

Regarding the simulation model of the hybrid controller, implementing a smooth transitioning function between controllers $\text{PID}_3$ and $\text{PID}_4$ could improve the performance. The controllers are structurally different, so the control input right before and right after a jump deviate, reducing the performance to some degree at these instances. It could also be advantageous to increase the simulation time in order to simulate the sea state change even more realistically.

The simplified vessel model, reference model with noise, giving input to the hybrid observers gives a good indication of the open loop performance of the observers. However, the observers' performance in closed loop with a controller and vessel should be conducted to see that they behave good in output feedback as well. The simulation model could also be extended to 3DOF so surge, sway and yaw can be estimated for a surface vessel in DP.

On the theoretical side, the stability analysis for both the controller and observers could be extended. For the hybrid controller the stability analysis has relied on the

separation principle, and left the observers $\text{NPO}_{1-4}$ out of the closed loop stability analysis. Obtaining a rigid stability proof for the entire system is suggested for further work.

The stability of the hybrid observers are discussed using set stability theory, and in addition stability of the first observer is completed using Lyapunov analysis. Using this to complete the Lyapunov analysis for observer 2, these results could at a later stage be extended to establish certain recurrence properties for systems with randomness by applying Lyapunov analysis tools developed in Teel (2013).

# Bibliography


Balchen, J. G., Jenssen, N. A., Mathisen, E., & Saelid, S. (1980). Dynamic Positioning of Floating Vessels Based on Kalman Filtering and Optimal Control. volume 2, (pp. 852–864).

Branicky, M. S. (1995). *Studies in Hybrid Systems; Modeling, Analysis and Control*. MiT, Cambridge, Masachusetts.

Brown, R. G. & Hwang, P. Y. C. (2012). *Introduction to Random Signals and Applied Kalman Filtering*. John Wiley & Sons, Inc.

DNV (2013). *Rules for Classification of Ships, Part 6 Chapter 7, Dynamic Positioning Systems*. DNV (Det Norske Veritas) AS.

DNV (2014). *DNV-RP-H103 Modelling and Analysis of Marine Operations*. DNV (Det Norske Veritas) AS.

Faltinsen, O. M. (1993). *Sea Loads on Ships and Offshore Structures*. Cambridge University Press.

Faltinsen, O. M. & Loken, A. E. (1979). Slow Drift Oscillations of a Ship in Irregular Waves. *Nor Veritas Publ*, (108).

Farrell, J. A., Givargis, T. D., & Barth, M. J. (2000). Real-time Differential Carrier Phase GPS-aided INS. *IEEE Transactions on Control Systems Technology*, *8*(4), 709–721.

Fjellstad, O.-E., Fossen, T. I., & Egeland, O. (1992). Adaptive Control of ROVs with Actuator Dynamics and Saturation. (pp. 513–522).

Fossen, T. I. (2011). *Handbook of Marine Craft Hydrodyamics and Motion Control*. Wiley.

Fossen, T. I. & Strand, J. P. (1999). Passive Nonlinear Observer Design for Ships using Lyapunov Methods: Full-scale Experiments with a Supply Vessel. *Automatica*, *35*(1), 3 – 16.

Goebel, R., Sanfelice, R. G., & Teel, A. R. (2012). *Hybrid Dynamical Systems, Modelling, Stability and Robustness*. Princeton University Press.

Hassani, V., Sørensen, A. J., & Pascoal, A. M. (2013). A Novel Methodology for Robust Dynamic Positioning of Marine Vessels: Theory and Experiments. *Proceedings of the American Control Conference*, 560–565.

Hespanha, J. P. (2002). Tutorial on Supervisory Control. Lecture notes for the workshop Control using Logic and Switching, 40th conf. on Decision and Control, Orlando Florida.

Hespanha, J. P., Liberzon, D., & Morse, A. S. (2003). Hysteresis-based Switching Algorithms for Supervisory Control of Uncertain Systems. *Automatica*, *39*(2), 263–272.

Hespanha, J. P. & Morse, A. S. (2002). Switching Between Stabilizing Controllers. *Automatica*, *38*(11), 1905–1917.

Hua, M.-D. (2010). Attitude Estimation for Accelerated Vehicles using GPS/INS Measurements. *Control Engineering Practice*, *18*(7), 723 – 732. Special Issue on Aerial Robotics.

Khalil, H. K. (2002). *Nonlinear Systems*. Prentice Hall, Upper Saddle River, NJ.

Loría, A., Panteley, E., Popovic, D., & Teel, A. (2002). An Extension of Matrosov's Theorem with Application to Stabilization of Nonholonomic Control Systems. volume 2, (pp. 1528–1533).

Matrosov, V. (1962). On the Stability of Motion. *Journal of Applied Mathematics and Mechanics*, *26*(5), 1337–1353.

Nguyen, T. D., Sørensen, A. J., & Quek, S. T. (2007). Design of Hybrid Controller for Dynamic Positioning from Calm to Extreme Sea Conditions. *Automatica*, *43*(5), 768–785.

Nguyen, T. D., Sørensen, A. J., & Quek, S. T. (2008). Multi-operational Controller Structure for Station Keeping and Transit Operations of Marine Vessels. *IEEE Transactions on Control Systems Technology*, *16*(3), 491–498.

Nocedal, J. & Wright, S. J. (2006). *Numerical Optimization*. Springer Science and Business Media, LLC.

Price, W. G. & Bishop, R. E. D. (1974). *Probalistic Theory of Ships*. Chapman and Hall, London.

Rockafellar, R. T. & Wets, R. J.-B. (2004). *Variational Analysis*. Springer-Verlag Berlin Heidelberg.

Sanfelice, R. G., Copp, D. A., & Ñañez, P. (2013). A Toolbox for Simulation of Hybrid Systems in Matlab/Simulink. *HSCC, Philadelphia, Pennsylvania, USA*.

Skjetne, R. (2005). The Maneuvering Problem, PhD Thesis. *Department of Marine Technology, NTNU*.

Smogeli, Ø. N. (2006). Control of Marine Propellers, from Normal to Extreme Conditions, PhD Thesis. *Department of Marine Technology, NTNU*.

Sørensen, A. (2011). A Survey of Dynamic Positioning Control Systems. *Annual Reviews in Control*, *35*(1), 123–136.

Sørensen, A. & Strand, J. (2000). Positioning of Small Waterplane-area Marine Constructions with Roll and Pitch Damping. *Control Engineering Practice*, *8*(2), 205–213.

Sørensen, A. J. (2005). Structural Issues in the Design and Operation of Marine Control Systems. *Annual Reviews in Control*, *29*(1), 125–149.

Sørensen, A. J. (2013). *Marine Control Systems, Propulsion and Motion Control of Ships and Ocean structures, Lecture Notes*. Department of Marine Technology, NTNU.

Sørensen, A. J., Strand, J. P., Nyberg, H., & Simrad, K. (2002). Dynamic Positioning of Ships and Floaters in Extreme Seas. *Oceans Conference Record (IEEE)*, *3*, 1850–1855.

Tannuri, E. A. & Morishita, H. M. (2006). Experimental and Numerical Evaluation of a Typical Dynamic Positioning System. *Applied Ocean Research*, *28*(2), 133–146.

Teel, A. (2013). Lyapunov Conditions Certifying Stability and Recurrence for a Class of Stochastic Hybrid Systems. *Annual Reviews in Control*, *37*(1), 1–24.

Titterton, D. H. & Weston, J. L. (1997). Stapdown Inertial Navigation Technology. *IEE. London, UK.*

Vik, B. & Fossen, T. I. (2001). Nonlinear Observer Design for Integration of GPS and Intertial Navigation Systems. *Proceedings of the Conference on Decision and Control (CDC'2001). Orlando, FL.*

# Paper 1

# Increasing the Operation Window for Dynamic Positioned Vessels Using the Concept of Hybrid Control

Astrid H. Brodtkorb, Asgeir J. Sørensen, Andrew R. Teel

To be published at the *ASME 2014 33rd International Conference on Ocean, Offshore and Arctic Engineering, OMAE 2014*

**Proceedings of the ASME 2014 33rd International Conference on Ocean, Offshore and Arctic Engineering**
**OMAE 2014**
**June 8-13, 2014, San Francisco, California, USA**

# OMAE2014-23601

# INCREASING THE OPERATION WINDOW FOR DYNAMIC POSITIONED VESSELS USING THE CONCEPT OF HYBRID CONTROL

**Astrid H. Brodtkorb**
Centre for Autonomous Marine Operations (AMOS),
Department of Marine Technology ,
Norwegian University of Science and Technology (NTNU),
Otto Nielsens vei 10, Trondheim, Norway
Email: astrbro@stud.ntnu.no

**Asgeir J. Sørensen**
Centre for Autonomous Marine Operations (AMOS),
Department of Marine Technology,
Norwegian University of Science and Technology (NTNU),
Otto Nielsens vei 10, Trondheim, Norway
Email: asgeir.sorensen@ntnu.no

**Andrew R. Teel**
Center for Control, Dynamical Systems, and Computation,
Department of Electrical Engineering,
University of California,
Santa Barbara, CA 93106-9560
Email: teel@ece.ucsb.edu

## ABSTRACT

In order to extend the operational window of marine vessels, the high-level control of the dynamic positioning (DP) system is revised. Major contributions of this paper include the modeling of a hybrid controller for a DP vessel in a varying sea state using the hybrid dynamical systems framework proposed by [1], and establishing global asymptotic stability of the closed-loop hybrid system. Simulations in a sea state varying from calm to extreme are conducted with the hybrid controller, and a single controller with adaptive wave filtering for comparison. The single controller becomes unstable in extreme seas whereas the hybrid controller shows good performance. Switching is based on spectral analysis of the vessel wave frequency motions.

## NOMENCLATURE

PID Proportional integral derivative controller
NPO Nonlinear passive observer
(U)GAS (Uniformly) globally asymptotically stable
$\boldsymbol{\eta}$ Generalized position vector including surge, sway, yaw
$\boldsymbol{\nu}$ Generalized velocity vector including surge, sway, yaw
$\mathbf{W}\boldsymbol{\xi}$ Wave frequency vessel motion, surge, sway, yaw
$\omega_p$ Peak wave frequency in the sea state
$\Upsilon(\boldsymbol{\chi})$ Estimated peak wave frequency in the sea state
$\omega_{p,m}$ Peak wave frequency in each observer $m = \{1,2,3,4\}$
$q$ Sea state estimate, $q = \{1,2,3,4\}$
$\mathscr{H}$ Hybrid system including hybrid controller and vessel

## INTRODUCTION

Oil and gas exploration and production activities are currently venturing into deeper waters resulting in an increasing number of subsea installations at the sea bed. Vessels with dynamic positioning (DP) capabilities are high in demand both due to their flexibility and good abilities to keep their position with high accuracy. With growing operational costs it is important that vessels on site can conduct operations even in harsher environmental conditions, thereby maximizing the operational window.

In normal operational conditions the first-order wave-induced motions of the vessel, usually with dominating wave excitation periods in the order of 5-10 seconds, are not compensated by the thrusters. This is achieved by filtering out the wave frequency response before the measurements enters the feedback controller. In extreme operational conditions the wavelengths and periods are longer, and the horizontal wave-induced motions of DP vessels become correspondingly larger. [2] eliminates the wave filter and achieves wave filtering with good results. Due to more prominent nonlinearities and couplings in the vessel response in extreme seas, the DP controllers for normal and extreme conditions could beneficially have different structures.

When the sea state changes, incorporating several controllers into one system could be beneficial for the performance. [3] used the switching systems framework [4–6] to design a hybrid DP controller for a vessel in a changing environment. A bank of controllers was designed together with a switch, and the sea state was monitored in a *supervisor* by estimating a peak wave frequency using spectral analysis. As the sea state progressed, the supervisor triggered switches between the controllers in the bank. A switching algorithm was implemented which ensured smooth switching and prevented *chattering*; the rapid switching back and forth between controllers, which may destabilize the system. The major findings were that the hybrid controller performed better than a single controller in sea states that vary from calm to extreme. It was also found that the proportional integral derivative (PID) controller with acceleration feedback reduced the standard deviation for both position and thrust in extreme seas compared with a PID controller without acceleration feedback.

[7] extended the same concepts to include models where the vessel was in maneuvering and transit modes in addition to stationkeeping. An integrated marine control system which allowed smooth switching between controllers for specific operations subject to differing environmental conditions yielded good results.

[1] presents a different hybrid framework which combines continuous and instantaneous change, and hence can describe many different types of systems, see [8]. Adopted for DP, the continuous states consist of position and velocity of the vessel (flow dynamics), and the discrete states include logic variables determining to which *mode*, when and how the continuous state should switch (jump dynamics). Stability and robustness results for systems in [1] are based on results for continuous-time nonlinear systems, see [9].

Inspired by [3, 7] the hybrid modeling framework proposed by [1] is adopted for a vessel in DP. The major contribution of this paper is using the modeling framework and stability results from [1] to model a hybrid DP controller for changing environmental condition. The flow dynamics include four nonlinear passive observers (NPO), four nonlinear PID controllers and a switch. A sea state estimate is calculated in the jump dynamics based on spectral analysis of the vessel wave frequency response. The sea state estimate $q = \{1,2,3,4\}$ indicates which sea state the vessel experiences, and the associated controller and observer are selected to control the vessel. Switching is constrained by the nature of the spectral analysis so chattering is avoided. Simulations of a DP vessel in a sea state changing from calm to extreme are done with two different controllers in feedback, the hybrid controller and a single controller with adaptive wave filtering. Results from the two simulations are discussed.

The paper is organized as follows: A simplified mathematical model of the DP vessel and a model-based observer are presented, before the DP control objective and control algorithm are established. The hybrid controller is modeled based on the previous sections, and global asymptotic stability of the hybrid controller and the DP vessel is established. The simulation setup and results are discussed, before the conclusion.

## MATHEMATICAL MODELING OF DP VESSEL

This section introduces a simplified mathematical model of a vessel in DP, which serves as a basis for the observer and controller design.

### Process Plant Model

A high fidelity mathematical model of the marine vessel can be described as a six degree of freedom (6DOF) nonlinear low-frequency model [10]:

$$\begin{aligned}\mathbf{M}\dot{\boldsymbol{\nu}} + \mathbf{C}_{RB}(\boldsymbol{\nu})\boldsymbol{\nu} + \mathbf{C}_A(\boldsymbol{\nu})_r\boldsymbol{\nu}_r + \mathbf{D}(\kappa,\boldsymbol{\nu}_r) + \mathbf{G}(\boldsymbol{\eta}) \\ = \boldsymbol{\tau}_{env} + \boldsymbol{\tau}_{thr},\end{aligned} \tag{1}$$

where $\mathbf{M}$ is the inertia matrix including added mass, $\mathbf{C}_{RB}$ and $\mathbf{C}_A$ are the rigid body and added mass Coriolis matrices, $\mathbf{D}(\kappa,\boldsymbol{\nu}_r) = \mathbf{D}_L + \mathbf{d}_{NL}(\boldsymbol{\nu}_r)$ is the damping matrix consisting of a linear and nonlinear term, $\mathbf{G}$ is the restoring matrix, and $\boldsymbol{\tau}_{env}$ and $\boldsymbol{\tau}_{thr}$ are the forces acting on the ship from the environment and thrusters. $\boldsymbol{\eta}$, $\boldsymbol{\nu}$, and $\boldsymbol{\nu}_r$ are the generalized position, velocity and relative velocity vectors. For detailed description of the coefficients and matrices, see [10].

### Control Plant Model

A control plant model is a simplified mathematical description, based on Egn. (1), containing only the main physical properties. Controllers and observers may include the control plant

model, so it needs to be computationally fast. For DP applications $\boldsymbol{\nu}, \boldsymbol{\nu}_r$ are assumed small ($\approx \mathbf{0}$), and the vessel motions occur mostly in the horizontal plane, so heave, roll and pitch motions are neglected, giving the 3DOF states; $\boldsymbol{\eta} = [x, y, \psi]^T$, $\boldsymbol{\nu} = [u, v, r]^T$. $\mathbf{G}(\boldsymbol{\eta})$ can be neglected in surge sway and yaw since there is no buoyancy in the horizontal plane. Using model reduction, adding bias and transforming position from the body-frame to the NED-frame[1] yields the following low frequency control plant model, Eqn. (2a,b):

$$\dot{\boldsymbol{\eta}} = \mathbf{R}(\psi)\boldsymbol{\nu}, \tag{2a}$$

$$\mathbf{M}\dot{\boldsymbol{\nu}} = -\mathbf{D}_L\boldsymbol{\nu} + \boldsymbol{R}^T(\psi)\mathbf{b} + \boldsymbol{u}, \tag{2b}$$

$$\mathbf{y} = \boldsymbol{\eta} + \mathbf{W}\boldsymbol{\xi} + \mathbf{v}; \tag{2c}$$

Stability of the hybrid system is established. where Eqn. (2a) is the 3DOF kinematics and $\mathbf{R}(\psi)$ is the rotation matrix. In Eqn. (2b) $\boldsymbol{u}$ is the control input and $\mathbf{b}$ is the bias, a variable containing unmodeled dynamics and slowly varying disturbances, for instance current, wave drift, and nonlinear damping. The stability analysis for the hybrid controller is done for the case when $\mathbf{b}$ is constant. Then, by standard robustness results for hybrid systems, see for example [1, Corollary 7.27], stability-like properties can be inferred for the case when $\mathbf{b}$ is slowly varying, which is the more realistic case. Egn. (2c) is the measurement equation containing low frequency motions $\boldsymbol{\eta}$, wave frequency motions $\mathbf{W}\boldsymbol{\xi}$, and measurement noise $\mathbf{v}$. $\mathbf{v}$ is assumed zero in the modeling and stability analysis.

### Modeling of Wave Frequency Motions

The measurements are assumed to have the form in Eqn. (2c) where $\mathbf{W} \in \mathbb{R}^{3\times 2}$ and $\boldsymbol{\xi} \in \mathbb{S}^1 \subset \mathbb{R}^2$ satisfies the simplified wave model

$$\dot{\boldsymbol{\xi}} = \omega_p \mathbf{J}\boldsymbol{\xi}, \qquad \mathbf{J} = \begin{bmatrix} 0 & 1 \\ -1 & 0 \end{bmatrix}. \tag{3}$$

This is an oscillator without damping. For wave frequency modeling driven by white noise including damping, see [10, 11].

The wave frequency vessel motion is used to generate a sea state estimate, so the measurements $\mathbf{y}$ are passed through a high-pass filter with state $\mathbf{z} \in \mathbb{R}^3$ and dynamics

$$\dot{\mathbf{z}} = -\lambda(\mathbf{z} - \mathbf{y}) \tag{4a}$$

$$\mathbf{y}_f := \mathbf{y} - \mathbf{z} \tag{4b}$$

where $\lambda > 0$. This gives the expected steady state measurement $\mathbf{y}_{ss} = \boldsymbol{\eta}^* + \mathbf{W}\boldsymbol{\xi}$, and the expected steady state response of $\mathbf{z}$, $\mathbf{z}_{ss}$

$$\mathbf{z}_{ss} = \boldsymbol{\eta}^* + \boldsymbol{\Pi}_f\boldsymbol{\xi} \tag{5a}$$

$$\omega_p\boldsymbol{\Pi}_f\mathbf{J} = -\lambda(\boldsymbol{\Pi}_f - \mathbf{W}) \tag{5b}$$

where the second equation has a solution since the spectra of $\omega_p\mathbf{J}$ and $-\lambda\mathbf{I}$ are disjoint. The expected steady state behavior of $\mathbf{y}_f$, $\mathbf{y}_{f,ss}$, is $\mathbf{W}_f\boldsymbol{\xi}$ where $\mathbf{W}_f := \mathbf{W} - \boldsymbol{\Pi}_f$.

### Observer

The output to be controlled is the low frequency surge, sway and yaw motions, $\boldsymbol{\eta}$. An observer is needed to filter out $\mathbf{W}\boldsymbol{\xi}$ and estimate the bias in Eqn. (2b), providing a state estimate $\hat{\boldsymbol{\eta}}$ which is fed back to the controller. A nonlinear passive observer (NPO) is chosen, see [11]. The advantage of a NPO is that the yaw dynamics do not need to be linearized, so the observer has a global stability result. In addition the tuning is simpler than for instance an extended Kalman filter[2] because there are less states to tune. Tuning the gains according to [11] yields the observer passive and globally exponentially stable with much faster dynamics than those of the vessel. These results are utilized in the stability analysis of the hybrid controller.

## CONTROL OBJECTIVE AND ALGORITHM

The control objective is for the vessel to keep position with minimal standard deviations from the set-point even in extreme sea states, while minimizing power consumption. This means that the error between the generalized position $\boldsymbol{\eta}$ and the reference $\boldsymbol{\eta}^*$, here a set-point, should converge to zero as time increases

$$\lim_{t\to\infty} \boldsymbol{\eta}(t) - \boldsymbol{\eta}^*(t) \to \mathbf{0}$$

subject to minimum energy consumption. The reference is the desired position and heading $\boldsymbol{\eta}^* = [x^*, y^*, \psi^*]^T$ in the NED reference frame. In addition in order to save fuel, wave compensation should not be done unless the sea state is extreme.

### Proposed Control Algorithm

A nonlinear PID control law is chosen, in accordance with [3]:

$$\mathbf{u} = -\mathbf{R}^T(\psi)\mathbf{K}_p(\hat{\boldsymbol{\eta}} - \boldsymbol{\eta}^*) - \mathbf{K}_d\hat{\boldsymbol{\nu}} - \mathbf{R}^T(\psi)\mathbf{K}_i\int_0^t(\hat{\boldsymbol{\eta}} - \boldsymbol{\eta}^*)dt - \mathbf{K}_a\hat{\dot{\boldsymbol{\nu}}}, \tag{6}$$

[1] The transformation of position in the BODY-frame to the NED(North East Down)-frame is according to [11]: $\boldsymbol{\nu}^n = \boldsymbol{R}(\boldsymbol{\Theta})\boldsymbol{\nu}^b$, where $\boldsymbol{\Theta}$ are the rotations roll, pitch and yaw.

[2] [12, 13] presents DP systems with extended Kalman filters.

where $\mathbf{K}_j, j = \{p,d,i,a\}$ are gain matrices to the corresponding terms, which are chosen so the control plant model is asymptotically stable. $(\hat{\boldsymbol{\eta}} - \boldsymbol{\eta}^*)$ is the difference between the estimated position and desired position, $\hat{\boldsymbol{v}}$ is the estimated velocity, $\hat{\dot{\boldsymbol{v}}}$ is the estimated acceleration, and $\boldsymbol{u}$ is the input control force. A backstepping technique is used to prove uniform global asymptotic stability (UGAS) of Eqn. (2a,b) and Eqn. (6), see Appendix A for details.

## HYBRID SYSTEM MODELING

Motivated by a marine vessel in a sea state varying with time, a hybrid controller using the hybrid dynamical systems framework [1] is designed in this section.

A sea state can be represented statistically by means of a significant wave height $H_s$ and a characteristic wave frequency, here the peak wave frequency $\omega_p$ is used, see [14] for details. Based on [14], four sea states $m = \{1,2,3,4\}$ are defined in Table 1, which serves as a simplified environment model for the design. One controller and one observer is designed for each sea state, and then switch between them as the sea state changes. An estimate of the sea state $q$ is obtained through spectral analysis of the wave frequency vessel response. $m,q \in \{1,2,3,4\} =: Q$. A conceptual diagram of the hybrid system is shown in Fig. 1.

**TABLE 1**. SEA STATE, CONTROLLER, OBSERVER AND SWITCHING SIGNAL OVERVIEW.

| Sea State $m$ | $H_{s,m}$ [m] | $\omega_{p,m}$ [rad/s] | Controller $m$ | Observer $m$ | $q$ |
|---|---|---|---|---|---|
| 1 Calm | 1.25 | 0.79 | $\text{PID}_1$ | $\text{NPO}_1$ | 1 |
| 2 Moderate | 5.66 | 0.615 | $\text{PID}_2$ | $\text{NPO}_2$ | 2 |
| 3 High | 9.5 | 0.429 | $\text{PID}_3$ | $\text{NPO}_3$ | 3 |
| 4 Extreme | 14.0 | $\leq 0.279$ | $\text{PID}_4$ (w/ AFB) | $\text{NPO}_4$ (no WF) | 4 |

### Modeling of the Controller Set

The four controllers $\text{PID}_{1-4}$ all use the nonlinear PID control algorithm Eqn. (6), where the difference between them are the controller gains $\mathbf{K}_{j,m},\ j = \{p,d,i,a\}\ m \in Q$. The gains are lowest for $\text{PID}_1$ and highest for $\text{PID}_4$, making the controllers progressively more aggressive. $\mathbf{K}_{a,m} = 0$ for $m = \{1,2,3\}$. In extreme sea states, acceleration feedback (AFB) is included in surge $(-\mathbf{K}_{a,4}\dot{\boldsymbol{v}})$, which changes $\mathbf{M}$ to $(\mathbf{M} + \mathbf{K}_{a,4})$ in the closed loop system when $q = 4$. The control input $\boldsymbol{u}_q$ is

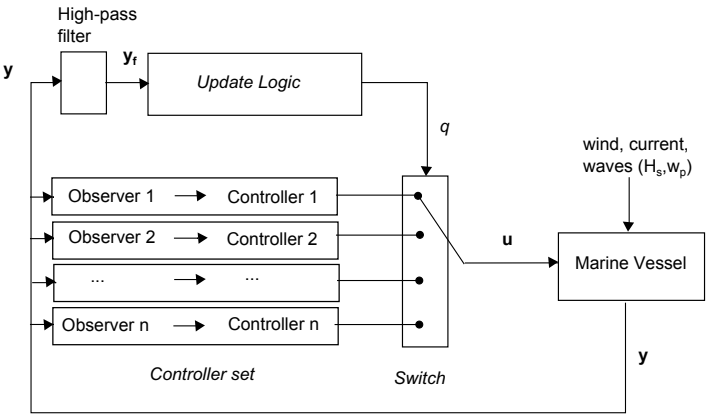


**FIGURE 1**. Conceptual diagram of the hybrid controller and marine vessel.

$$\dot{\boldsymbol{\zeta}} = \hat{\boldsymbol{\eta}}_q - \boldsymbol{\eta}^*, \tag{7a}$$

$$\boldsymbol{u}_q = -\boldsymbol{R}^T(\psi)\boldsymbol{K}_{p,q}(\hat{\boldsymbol{\eta}}_q - \boldsymbol{\eta}^*) - \boldsymbol{K}_{d,q}\hat{\boldsymbol{v}}_q - \boldsymbol{R}^T(\psi)\boldsymbol{K}_{i,q}\boldsymbol{\zeta} - \boldsymbol{K}_{a,q}\hat{\dot{\boldsymbol{v}}}_q, \tag{7b}$$

$$\hat{\boldsymbol{\eta}}_q = \boldsymbol{\eta} + \mathbf{W}_{observer,q}\boldsymbol{\xi}. \tag{7c}$$

where $q \in Q$ and the observer estimate is modeled as the low frequency vessel motion plus a wave-frequency residual $\mathbf{W}_{observer,q}\boldsymbol{\xi}$ dependent on the peak wave frequency in the observer.

The four observers $\text{NPO}_{1-4}$ are designed and tuned using tuning laws in [11]. The observers have a peak frequency $\omega_{p,m},\ m \in Q$ in the wave filters, corresponding to each predefined sea state, i.e. $\omega_{p,1} = 0.79,\ \omega_{p,2} = 0.615,\ \omega_{p,3} = 0.429$, and $\omega_{p,4} = 0.279$. The observer estimate in feedback $\hat{\boldsymbol{\eta}}_q$ is expressed in Eqn. (7c). It is further assumed that

**Assumption 1:**

a) When $q \equiv m$, then $\mathbf{W}_{observer,m} = 0$, giving $\hat{\boldsymbol{\eta}} = \boldsymbol{\eta}$
b) For the case where $q \equiv m$ then the closed-loop system Eqn. (2) and Eqn. (7) has the point $(\boldsymbol{\eta}^*, \mathbf{0}, \mathbf{K}_{i,m}^{-1}\mathbf{b})$ UGAS
c) Under arbitary switching of $q$, there are no finite escape times ■

Point a) follows from the observer dynamics, see [11], where the estimates converge asymptotically to the states. In Appendix A, point b) is verified by establishing UGAS of the closed-loop system Eqn.(2) and Eqn. (6), which is valid for all controllers. Point c) refers to when $q \neq m$, which implies there are wave frequency components in the feedback signal. This leads to the thrusters compensating for waves using more power then necessary, but without influencing stability.

### Modeling the Update Logic for $q$

In this section, the update dynamics of the sea state estimate $q \in Q \subset \mathbb{R}$ is discussed. The output $\mathbf{y}_f$ of the high-pass filter from the section on wave frequency modeling is sampled every $T > 0$ seconds and $N \in \mathbb{Z}_{\geq 1}$ consecutive measurements are stored in the state of a shift register with state $\boldsymbol{\chi} \in \mathbb{R}^{3N}$, where $\boldsymbol{\chi}_i \in \mathbb{R}^3$, $i \in \{1,\ldots,N\}$ are the stored measurements. The state component $\boldsymbol{\chi}_1$ contains the most recent sample, and $\boldsymbol{\chi}_N$ contains the least recent sample, see Eqns. (9a-f).

Spectral analysis is applied to $\boldsymbol{\chi}$ in order to estimate the sea state peak frequency. The function $\Upsilon : \mathbb{R}^{3N} \to \mathbb{R}_{\geq 0}$ denotes the function that operates on $\boldsymbol{\chi}$ and returns a frequency $\Upsilon(\boldsymbol{\chi})$ corresponding to the largest frequency component in the specter of $\boldsymbol{\chi}$. The value of $\Upsilon(\boldsymbol{\chi})$ is compared to the four frequencies $\omega_{p,m}$, $m \in Q$, and $q$ is updated to any value $q \in Q$ that minimizes $|\Upsilon(\boldsymbol{\chi}) - \omega_{p,q}|$.

Let $\tau \in \mathbb{R}$ be a timer that triggers the update of the states of $\boldsymbol{\chi}$, which occurs every $T > 0$ seconds. Let $\ell \in \mathbb{R}$ be a counter that triggers when the estimate of $q$ is updated, which occurs every $LT$ seconds where $L \in \mathbb{Z}_{\geq 1}$. The jumps for these variables are allowed when

$$(\boldsymbol{\eta}, \boldsymbol{\nu}, \boldsymbol{\zeta}, \boldsymbol{\xi}, \mathbf{z}, \boldsymbol{\chi}, \tau, \ell, q) \in D := \mathbb{R}^3 \times \mathbb{R}^3 \times \mathbb{R}^3 \times \mathbb{S}^1 \times \mathbb{R}^3 \times \mathbb{R}^{3N} \times \{T\} \times \{0,\ldots,L\} \times Q \tag{8}$$

and the jumps satisfy

$$\boldsymbol{\chi}_1^+ = \mathbf{y}_f \tag{9a}$$
$$\boldsymbol{\chi}_2^+ = \boldsymbol{\chi}_1 \tag{9b}$$
$$\vdots \tag{9c}$$
$$\boldsymbol{\chi}_N^+ = \boldsymbol{\chi}_{N-1} \tag{9d}$$
$$\tau^+ = 0 \tag{9e}$$
$$\ell^+ = \begin{cases} \ell + 1 & \ell \in \{0,\ldots,L-1\} \\ 0 & \ell = L \end{cases} \tag{9f}$$
$$q^+ \in \begin{cases} q & \ell \in \{0,\ldots,L-1\} \\ \arg\min_{\alpha \in Q} |\Upsilon(\boldsymbol{\chi}) - \omega_{p,\alpha}| & \ell = L. \end{cases} \tag{9g}$$

All of the states introduced in this section remain constant during flows, except for $\tau$ which satisfies $\dot{\tau} = 1$. Flows are allowed when

$$(\boldsymbol{\eta}, \boldsymbol{\nu}, \boldsymbol{\zeta}, \boldsymbol{\xi}, \mathbf{z}, \boldsymbol{\chi}, \tau, \ell, q) \in C := \mathbb{R}^3 \times \mathbb{R}^3 \times \mathbb{R}^3 \times \mathbb{S}^1 \times \mathbb{R}^3 \times \mathbb{R}^{3N} \times [0,T] \times \{0,\ldots,L\} \times Q. \tag{10}$$

The hybrid model of the sea state updates can be compactly written as

$$(\boldsymbol{\xi}, \boldsymbol{\chi}, \tau) \in \mathbb{S}^1 \times \mathbb{R}^{3N} \times [0,T] \quad \begin{cases} \dot{\boldsymbol{\xi}} &= \omega_p \mathbf{J} \boldsymbol{\xi} \\ \dot{\boldsymbol{\chi}} &= \mathbf{0} \\ \dot{\tau} &= 1 \end{cases} \tag{11a}$$

$$(\boldsymbol{\xi}, \boldsymbol{\chi}, \tau) \in \mathbb{S}^1 \times \mathbb{R}^{3N} \times \{T\} \quad \begin{cases} \boldsymbol{\xi}^+ &= \boldsymbol{\xi} \\ \boldsymbol{\chi}^+ &= \mathbf{A}\boldsymbol{\chi} + \mathbf{B}\mathbf{W}_f \boldsymbol{\xi} \\ \tau^+ &= 0. \end{cases} \tag{11b}$$

It is used that $\mathbf{y}_{f,ss} = \mathbf{W}_f \boldsymbol{\xi}$, and the matrices $\mathbf{A}$ and $\mathbf{B}$ are derived from the equations given above for $\boldsymbol{\chi}^+$.

The expected steady-state response for $\boldsymbol{\chi}$, denoted $\boldsymbol{\chi}_{ss}$, can be verified to be

$$\boldsymbol{\chi}_{ss} = \boldsymbol{\Pi}(\tau)\boldsymbol{\xi} \tag{12a}$$
$$\dot{\boldsymbol{\Pi}}(\tau) = -\omega_p \boldsymbol{\Pi}(\tau)\mathbf{J} \tag{12b}$$
$$\mathbf{A}\boldsymbol{\Pi}(T) + \mathbf{B}\mathbf{W}_f = \boldsymbol{\Pi}(0). \tag{12c}$$

In order to assert that $q = m$ is the expected steady state response of $q$, it is assumed that

**Assumption 2** The function $\Upsilon$ is continuous and

$$\arg\min_{\alpha \in Q} |\Upsilon(\boldsymbol{\Pi}(T)\boldsymbol{\xi}) - \omega_{p,\alpha}| = m \qquad \forall \boldsymbol{\xi} \in \mathbb{S}^1 \,.$$

■

Under this assumption, the steady-state behavior for $q$, denoted $q_{ss}$, is that $q_{ss} = m$, since the steady-state $\boldsymbol{\chi}_{ss}$ at jumps is $\boldsymbol{\Pi}(T)\boldsymbol{\xi}$. $\boldsymbol{\Pi}(T)\boldsymbol{\xi}$ corresponds to samples of a steady-state signal that has frequency components only at the frequency $\omega_p$.

The spectral analysis method applied to $\boldsymbol{\chi}$ must satisfy Assumption 2. The discrete Fourier transform (DFT) does this. The DFT of $\boldsymbol{\Pi}(T)\boldsymbol{\xi}$ returns coefficients reflecting the intensity of each frequency in the samples. Since $\boldsymbol{\Pi}(T)\boldsymbol{\xi}$ contains only one frequency $\omega_p$, this has the highest intensity, and is returned by $\Upsilon(\boldsymbol{\chi})$. If the sea state is $\omega_{p,m}$, then the peak frequency returned by the DFT is $\Upsilon(\boldsymbol{\chi}) = \omega_{p,m}$, and hence the sea state estimate $q = m$.

**Remark** For sea spectra with double peaks, $\Upsilon(\boldsymbol{\chi})$ returns the lowest frequency corresponding to swell. This ensures compensation for swell motions.

The hybrid controller and vessel is referred to as the hybrid system $\mathscr{H}$, defined by Eqns. (2a,b), (7), and (11). $\mathscr{H}$ jumps when the states are in Eqn. (8) and flows when the states are in Eqn. (10).

## STABILITY ANALYSIS OF THE HYBRID SYSTEM

The stability analysis in this section is expanded to include the jump dynamics, and therefore the stability of a set is discussed.

### The Attractor $\mathscr{A}$

The set is the attractor of the hybrid system $\mathscr{H}$, and is derived from the expected steady-state analysis of the previous sections. In particular, for the overall hybrid system with state

$$(\boldsymbol{\eta},\boldsymbol{\nu},\boldsymbol{\zeta},(\boldsymbol{\xi},\mathbf{z},\boldsymbol{\chi},\tau),\ell,q) \in \mathbb{R}^3\times\mathbb{R}^3\times\mathbb{R}^3\times (\mathbb{S}^1\times\mathbb{R}^3\times\mathbb{R}^{3N}\times\mathbb{R})\times\mathbb{R}\times\mathbb{R} \quad (13)$$

the set to be analyzed is

$$\mathscr{A} := \{\boldsymbol{\eta}^*\}\times\{\mathbf{0}\}\times\left\{\mathbf{K}_{i,m}^{-1}\mathbf{b}\right\}\times\Psi\times\{0,\ldots,L\}\times\{m\}. \quad (14)$$

where

$$\Psi := \big\{(\boldsymbol{\xi},\mathbf{z},\boldsymbol{\chi},\tau)\in\mathbb{S}^1\times\mathbb{R}^3\times\mathbb{R}^{3N}\times[0,T]: \mathbf{z}=\boldsymbol{\eta}^*+\boldsymbol{\Pi}_f\boldsymbol{\xi},\boldsymbol{\chi}=\boldsymbol{\Pi}(\tau)\boldsymbol{\xi}\big\} \quad (15)$$

with $\boldsymbol{\Pi}_f$ defined via Eqn. (5b) and $\boldsymbol{\Pi}(\tau)$ defined via Egns. (12b)-(12c).

### Stability

Proposition [1, Prop. 7.5] can be used to prove asymptotic stability of the set $\mathscr{A}$, (14-15). It is expressed in terms of the following concepts:

A set $\mathscr{A}$ is *strongly forward invariant* if every maximal solution $\phi$ starting in $\mathscr{A}$ has range in a subset of $\mathscr{A}$, see [1, Def. 6.25].

A compact set $\mathscr{A}$ is *uniformly attractive* for a set $S\subset\mathbb{R}^n$ if every maximal solution $\phi$ is bounded and for every $\varepsilon>0$ there exists a $T>0$ such that $|\phi(t,j)|_{\mathscr{A}}\le\varepsilon$ for every maximal solution $\phi$ and $(t,j)\in$ dom $\phi$ with $t+j\ge T$, see [1, Def. 6.24].

**Proposition 1 [1, Prop. 7.5 and Def. 7.5])** Stability from invariance plus uniform convergence.
(a) Let the hybrid system $\mathscr{H}$ be nominally well-posed.
(b) Suppose that a compact set $\mathscr{A}\subset\mathbb{R}^n$ has the following properties:

i. it is strongly forward invariant, and
ii. is it uniformly attractive from a neighborhood of itself, ie. there exists a $\mu>0$ such that $\mathscr{A}$ is uniformly attractive from $\mathscr{A}+\mu\mathbb{B}$
iii. the basin of attraction of $\mathscr{A}$, denoted $\mathscr{B}^p_{\mathscr{A}}$, is the set of points $\xi\in\mathbb{R}^n$ such that every solution $\phi$ to $\mathscr{H}$ with $\phi(0,0)=\xi$ is bounded, and if it is complete, then also $\lim_{t+j\to\infty}|\phi(t,j)|_{\mathscr{A}}=0$.

Then the compact set $\mathscr{A}$ is globally asymptotically stable. ■

*Nominally well-posedness* is satisfied if the hybrid system satisfy the hybrid basic conditions, see [1, Assumption 6.4]. These are:

(A1) $C$ and $D$ are closed subsets of $\mathbb{R}^n$;
(A2) The set-valued mapping $F:\mathbb{R}^n\rightrightarrows\mathbb{R}^n$ is outer semi-continuous[3] (OSC) and locally bounded relative to $C$, $C\subset$ dom $F$, and $F(\mathbf{x})$ is convex for every $\mathbf{x}\in C$;
(A3) The set-valued mapping $G:\mathbb{R}^n\rightrightarrows\mathbb{R}^n$ is OSC and locally bounded relative to $D$, and $D\subset$ dom $G$.

### Applying Proposition 1 to the Hybrid System $\mathscr{H}$ and Set $\mathscr{A}$

(a) $\mathscr{H}$ is shown to be well-posed in Appendix B.
(b) $\mathscr{A}$ is compact because the components are closed and bounded sets.

### Forward invariance

The next proposition follows from the steady-state analysis above.

**Proposition 2** Under Assumptions 1 and 2, the set $\mathscr{A}$ defined in Eqns. (14)-(15) is forward invariant. ■

### Uniform global attractivity

**Assumption 3** For each compact set $K\subset\mathbb{R}^{17+3N}$, there exists $M>0$ such that, for each solution $\phi$ starting in $K$ and each $(t,j)\in$ dom $\phi$ for which $t+j\ge M$ we have that $q(t,j)=m$. ■
This assumption is plausible, at least for linear dynamics, since the steady-state response for $\mathbf{y}_f$, even under the wrong controller, should just have frequency components at $\omega_p$.

**Theorem 1** Under Assumptions 1-3, the set $\mathscr{A}$ satisfies Proposition 1 and is globally asymptotically stable.

**Sketch of Proof** Proposition 2 says that the set $\mathscr{A}$ defined in Eqns. (14)-(15) is forward invariant under Assumptions

[3] A set-valued mapping is OSC if for each convergent sequence $\{(x_i,y_i)\}_{i=1}^{\infty}$ that satisfies $y_i\in H(x_i),\forall i\ge 1$ and the limit denoted (x,y) satisfies $y\in H(x)$. If $f:C\to\mathbb{R}^n$ is continuous and C is closed, the the set-valued mapping $F:\mathbb{R}^n\rightrightarrows\mathbb{R}^n$ given by $F(x)=f(x)$ for x in C and $F(x)=\emptyset$ otherwise, is OSC.

1 and 2. In order to fulfill Proposition 1, uniform convergence from each compact set $K \subset \mathbb{R}^{17+3N}$ is needed. There are no finite escape times due to Assumption 1. Let $M > 0$ come from Assumption 3. Since the system is well-posed, the reachable set in time $M+1$ is compact. Denote this set $K_2$. Consider the behavior of the solution restarting at a time $(s,i)$ such that $s+i \in [M, M+1]$ and such that $q(t,j) = m$ for all $(t,j)$ in the domain of the solution such that $t+j \geq s+i$. According to Assumption 1 and the linear dynamics of the remaining states, the solution converges uniformly toward $\mathscr{A}$ from $K_2$. That is, for each $\varepsilon > 0$ there exists $M_2$ such that $t+j \geq M+1+M_2$ implies that the solution $\phi$ satisfies $|\phi(t,j)|_{\mathscr{A}} \leq \varepsilon$. ■

## SIMULATION RESULTS AND DISCUSSION

The numerical simulation is performed in Matlab/Simulink using a process plant model, see Eqn. (1), based on the work in [15] among others. The simulated vessel has $L_{pp,\ model} = 1.97m$ and is a model of a Platform Supply Vessel (PSV) $L_{pp,\ full-scale} = 68m$. The thruster configuration is shown in Fig. 2.

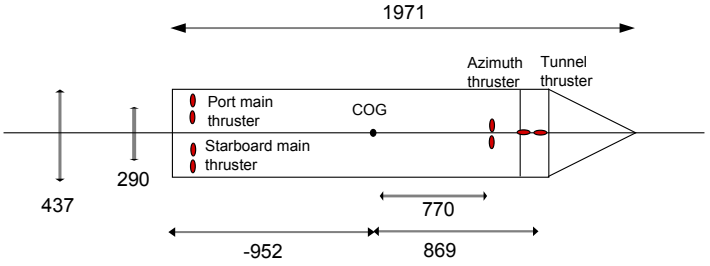


**FIGURE 2**. THRUSTER CONFIGURATION FOR MODEL SHIP, [mm].

### Setup

The hybrid controller is implemented into Matlab/Simulink. The controllers and observers are fine-tuned to give best performance in one pre-defined sea state, see Table 1. Note that the values for $H_{s,m}$ and $\omega_{p,m}$ given in Table 1 are full-scale values, which are scaled down to model-scale in the simulations. Two simulation scenarios for the vessel are presented for a sea state changing from calm to extreme. The first shows the performance of a single PID controller with adaptive wave filtering [16], and the second shows performance when the hybrid controller switching between $\text{PID}_{1-4}$. The single controller uses $\Upsilon(\boldsymbol{\chi})$ in the wave filter of the observer, and has controller gains like $\text{PID}_1$.

The simulated sea state consists of waves, mean wind, wind gusts and current, all of which are bow incident. Irregular waves are generated for $(H_s, \omega_p)$ by summing 50 harmonic wave components with frequencies computed using the JONSWAP spectrum and random wave phases. Increasing $H_s$ and decreasing $\omega_p$ in intervals as the simulation progresses, simulates a sea state changing from calm to extreme. In Fig. 5 the input $\omega_p$ to the wave generation is shown in red. The current and mean wind velocities increase with the simulation time.

At the beginning of the simulation, the waves may have transients due to initialization. The sea state is allowed to settle for 500 seconds, which is a lot longer than the build up time of the sea state, before changing $(H_s, \omega_p)$. The change from one sea state to another is done using a ramp function in 0.2 seconds, which is almost like a step. Because $\Delta\omega_p = 0.135$ and $\Delta H_s = 0.0148$ are small, the transient effects of the change are also assumed small. The sea state estimate is in these simulations based on $N = 2048$ number of measurements taken with a sampling period of $T = 0.1826$ seconds. The update is triggered when $L = 2048$, which implies no overlap in the measurements when doing a new spectral analysis.

### Results and Discussion

The simulation results for the single controller and hybrid controller are presented in Fig. 3 and Fig. 4. The sea state estimate $q$ and the estimated peak frequency $\Upsilon(\boldsymbol{\chi})$ in the sea state for the hybrid controller are shown in Fig. 5.

The single controller with adaptive wave filtering becomes unstable when the sea state enters the extreme regime. Instability is caused when the estimated peak frequency $\Upsilon(\boldsymbol{\chi})$

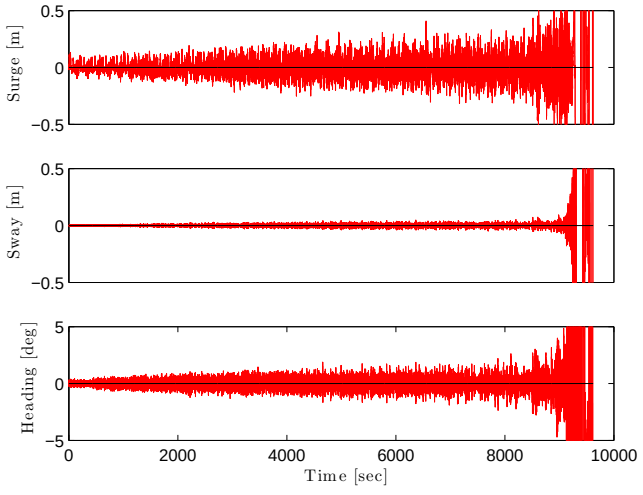


**FIGURE 3**. SINGLE CONTROLLER PERFORMANCE IN SEA STATE VARYING FROM CALM TO EXTREME.

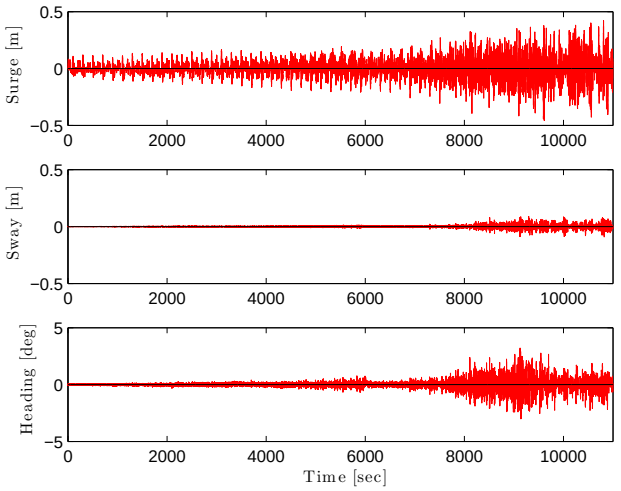


**FIGURE 4**. HYBRID CONTROLLER PERFORMANCE IN SEA STATE VARYING FROM CALM TO EXTREME.

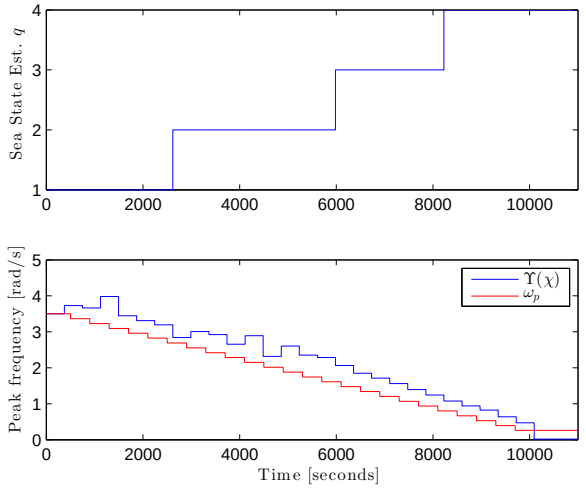


**FIGURE 5**. SEA STATE ESTIMATE $q$, ESTIMATED PEAK FREQUENCY $\Upsilon(\boldsymbol{\chi})$, AND PEAK FREQUENCY $\omega_P$ IN THE SIMULATED SEA STATE.

approaches zero, see Fig. 5, resulting in the observer filtering out wave frequency and low frequency motions before the measurements enter the feedback controller. This leads to poor controller performance. As a result the simulation is aborted before the simulation end-time, as the vessel position is -2500 meters in surge and 250 meters in sway, and has large rotations in yaw.

The hybrid controller is stable for the entire simulation time, see Fig. 4, and the switching is also stable, see Fig. 5. The position and thrust variance, given in Table 2, are fairly small considering the rough conditions towards the end. However comparing these results to the single controller is not meaningful due to the stability problems of the latter. The maximum thrust in surge of the vessel is $\pm 10$ $[N]$, and the mean commanded thrust in surge is $-7.492$ $[N]$. Adding smooth transitions between $\text{PID}_3$ and $\text{PID}_4$ could improve the performance in the region around 7500 seconds. This is subject to further research.

**TABLE 2**. SIMULATION STATISTICS, POSITION AND COMMANDED THRUST.

| Hybrid Controller | | | |
|---|---|---|---|
| | Surge | Sway | Yaw |
| Mean position [$10^{-3}$m], [deg] | 0.2446 | 0.0204 | -0.0141 |
| Position variance [$m^2$], [$deg^2$] | 0.0758 | 0.0101 | 0.0066 |
| Mean thrust [N], [Nm] | -0.7492 | 0.0039 | 0.0029 |
| Thrust variance [$N^2$], [$(Nm)^2$] | 0.7613 | 0.3221 | 0.0665 |

The estimated peak frequency $\Upsilon(\boldsymbol{\chi})$ in the sea state is slightly higher than the simulation input $\omega_p$, see Fig. 5. This is because $\Upsilon(\boldsymbol{\chi})$ is based on the vessel wave frequency motions and not the incident waves. In the beginning of the simulation, $\Upsilon(\boldsymbol{\chi})$ overestimates $\omega_p$ the most. This is because at higher incident wave frequencies the vessel response is smaller, making $\mathbf{W}\boldsymbol{\xi}$ more prone to noise. After 10000 seconds, $\Upsilon(\boldsymbol{\chi})$ drops to zero because $\text{PID}_4$ compensates for the wave frequency motions, and thus $\mathbf{W}\boldsymbol{\xi} = \mathbf{0}$. The way of tracking the sea state seems to work well in this application, and problems with the abrupt change in $(H_s, \omega_p)$ were not encountered. The length of the time-series to convert to the frequency domain is in this simulation $N = 2048$ and with no overlapping measurements. The results are also good with $N = 1024$, but in this case the controller switches back and forth a couple of times at the transitions. Because the sea state in reality varies slowly, doubling $N$ shows little influence on the system. The sample-hold behavior of $\Upsilon(\boldsymbol{\chi})$ introduces hysteresis switching on the system.

## CONCLUSION

The hybrid controller performed better than a single controller when the sea state changes from calm to extreme. As expected the single controller with adaptive wave filtering became unstable in extreme seas due to filtering of low frequency vessel motions.

Using spectral analysis in surge, sway and yaw to estimate the sea state seemed to work well, and in these simulations instability due to switching was not detected. The behavior of $\Upsilon(\boldsymbol{\chi})$ acts as a hysteresis switching constraint on the system.

## ACKNOWLEDGMENT

This work was supported by the Research Council of Norway through the Centres of Excellence funding scheme, project number 223254 – AMOS, and in part by AFOSR grant FA9550-12-1-0127, and NSF grant ECCS-1232035.

## REFERENCES

[1] Goebel, R., Sanfelice, R. G., and Teel, A. R., 2012. *Hybrid Dynamical Systems, Modeling, Stability and Robustness*. Princeton University Press.

[2] Sørensen, A. J., Strand, J. P., and Nyberg, H., 2002. "Dynamic positioning of ships and floaters in extreme seas". *Oceans Conference Record (IEEE),* ***3***, pp. 1850–1855.

[3] Nguyen, T. D., Sørensen, A. J., and Quek, S. T., 2007. "Design of hybrid controller for dynamic positioning from calm to extreme sea conditions". *Automatica,* ***43***(5), pp. 768–785.

[4] Hespanha, J. P., 2002. Tutorial on supervisory control. Lecture notes for the workshop Control using Logic and Switching, 40th conf. on Decision and Control, Orlando Florida.

[5] Hespanha, J. P., and Morse, A. S., 2002. "Switching between stabilizing controllers". *Automatica,* ***38***(11), pp. 1905–1917.

[6] Hespanha, J. P., Liberzon, D., and Morse, A. S., 2003. "Hysteresis-based switching algorithms for supervisory control of uncertain systems". *Automatica,* ***39***(2), pp. 263–272.

[7] Nguyen, T. D., Sørensen, A. J., and Quek, S. T., 2008. "Multi-operational controller structure for station keeping and transit operations of marine vessels". *IEEE Transactions on Control Systems Technology,* ***16***(3), pp. 491–498.

[8] Branicky, M. S., 1995. *Studies in Hybrid Systems; Modeling, Analysis and Control*. MiT, Cambridge, Masachusetts.

[9] Khalil, H. K., 2002. *Nonlinear Systems*. Prentice Hall, Upper Saddle River, NJ.

[10] Sørensen, A. J., 2013. *Marine Control Systems, Propulsion and Motion Control of Ships and Ocean structures, Lecture Notes*. Department of Marine Technology, NTNU.

[11] Fossen, T. I., 2011. *Handbook of Marine Craft Hydrodyamics and Motion Control*. Wiley.

[12] Tannuri, E., and Morishita, H., 2006. "Experimental and numerical evaluation of a typical dynamic positioning system". *Applied Ocean Research,* ***28***(2), pp. 133–146. cited By (since 1996)39.

[13] Hassani, V., Sørensen, A., and Pascoal, A., 2013. "A novel methodology for robust dynamic positioning of marine vessels: Theory and experiments". pp. 560–565.

[14] Price, W. G., and Bishop, R. E. D., 1974. *Probalistic Theory of Ships*. Chapman and Hall, London.

[15] Smogeli, Ø. N., 2006. *Control of Marine Propellers, From Normal to Extreme Conditions, PhD Thesis*. Department of Marine Technology, NTNU.

[16] Strand, J. P., and Fossen, T. I., 1999. *Nonlinear Passive Observer for Ships with Adaptive Wave Filtering, (In New Directions in Nonlinear Observer Design)*. Springer-Verlag London Ltd.

[17] Skjetne, R., 2005. *The Maneuvering Problem, PhD Thesis*. Department of Marine Technology, NTNU.

[18] Loría, A., Panteley, E., Popovic, D., and Teel, A., 2002. "An extension of Matrosov's theorem with application to stabilization of nonholonomic control systems". Vol. 2, pp. 1528–1533.

## Appendix A: Stability Analysis of Controllers $\text{PID}_{1-4}$

Stability of Eqn. (2a,b) and Eqn. (6) is analyzed using Lyapunov functions. The stability result of the NPO is used, see [11], where the estimates converge asymptotically to the states; $\hat{\boldsymbol{\eta}} \to \boldsymbol{\eta}$, $\hat{\boldsymbol{\nu}} \to \boldsymbol{\nu}$, $\hat{\boldsymbol{b}} \to \boldsymbol{b}$. In order to prepare for the analysis $\dot{\boldsymbol{R}}(\psi)$ is calculated:

$$\dot{\boldsymbol{R}}(\psi) = \mathbf{R}^x \dot{x} + \mathbf{R}^y \dot{y} + \mathbf{R}^\psi \dot{\psi} = \mathbf{R}^\psi \dot{\psi} = \mathbf{R}(\psi)\mathbf{S}r, \tag{16a}$$

where $\mathbf{S} = \begin{bmatrix} 0 & -1 & 0 \\ 1 & 0 & 0 \\ 0 & 0 & 0 \end{bmatrix}$. The notation $\mathbf{R}^j$ is adapted from [17], and it is the short form of $\frac{\partial \mathbf{R}}{\partial j}$.

**Step 1: Stabilizing the kinematics** New states are introduced in order to simplify the stability analysis:

$$\mathbf{z}_1 := \mathbf{R}^T(\psi)(\boldsymbol{\eta} - \boldsymbol{\eta}^*(t)), \tag{17a}$$

$$\tilde{\boldsymbol{\zeta}} := \mathbf{R}^T(\psi)(\boldsymbol{\zeta} - \mathbf{K}_i^{-1}\mathbf{b}), \tag{17b}$$

$$\mathbf{z}_2 := \boldsymbol{\nu} - \boldsymbol{\alpha}_1(\boldsymbol{\eta}, t), \tag{17c}$$

where $\boldsymbol{\eta}^*(t)$ is the desired position $(x^*, y^*)$ and heading $\psi^*$ which is assumed continuously differentiable provided by a guidance system. $\boldsymbol{\alpha}_1(\boldsymbol{\eta}, t)$ is the virtual control input which will be used in the design, and $\tilde{\boldsymbol{\zeta}}$ is the integral state, $\mathbf{K}_i = \mathbf{K}_i^T > 0$ and $\dot{\tilde{\boldsymbol{\zeta}}} = \mathbf{z}_2$.

Differentiating $\mathbf{z}_1$ with respect to time gives $\dot{\boldsymbol{z}}_1 =$

$-r\mathbf{S}\mathbf{z}_1 + \boldsymbol{\nu} - \mathbf{R}^T(\psi)\dot{\boldsymbol{\eta}}^*(t)$. The proposed Control Lyapunov function (CLF) is

$$\mathbf{V}_1 = \frac{1}{2}\mathbf{z}_1^T\mathbf{z}_1, \tag{18}$$

which is a positive definite function satisfying $\mathbf{V}_1(\mathbf{z}_1) \neq \mathbf{0} \quad \forall \mathbf{z}_1 \neq \mathbf{0}$, $\mathbf{V}_1(\mathbf{z}_1) = \mathbf{0}\ \forall \mathbf{z}_1 = \mathbf{0}$ . Differentiating $\mathbf{V}_1$ and using relation (17c) for $\boldsymbol{\nu}$ gives

$$\dot{\mathbf{V}}_1 = \mathbf{z}_1^T\dot{\mathbf{z}}_1 = \mathbf{z}_1^T[-r\mathbf{S}\mathbf{z}_1 + \boldsymbol{\alpha}_1(\boldsymbol{\eta},t) - \mathbf{R}^T(\psi)\dot{\boldsymbol{\eta}}^*(t)] + \mathbf{z}_1^T\mathbf{z}_2.$$

Choosing the virtual control input as

$$\boldsymbol{\alpha}_1(\boldsymbol{\eta},t) = \mathbf{R}^T(\psi)\dot{\boldsymbol{\eta}}^*(t) + r\mathbf{S}\mathbf{z}_1 - \mathbf{Q}_1\mathbf{z}_1, \tag{19}$$

where $\mathbf{Q}_1 = \mathbf{Q}_1^T > \mathbf{0}$, gives

$$\dot{\mathbf{V}}_1 = -\mathbf{z}_1^T\mathbf{Q}_1\mathbf{z}_1 + \mathbf{z}_1^T\mathbf{z}_2. \tag{20}$$

$\dot{\boldsymbol{\alpha}}_1$ is needed in the next step, and is

$$\dot{\boldsymbol{\alpha}}_1 = \dot{\mathbf{R}}^T(\psi)\dot{\boldsymbol{\eta}}^*(t) + \mathbf{R}^T(\psi)\ddot{\boldsymbol{\eta}}^*(t) + \dot{r}\mathbf{S}\mathbf{z}_1 + (r\mathbf{S} - \mathbf{Q}_1)\dot{\mathbf{z}}_1. \tag{21}$$

**Step 2: Stabilizing the whole system** Differentiating $\mathbf{z}_2$ from Eqn. (17c) with respect to time gives $\dot{\mathbf{z}}_2 = \mathbf{M}^{-1}[-\mathbf{D}_L\boldsymbol{\nu} + \boldsymbol{R}^T(\psi)\mathbf{b} + \mathbf{u}] - \dot{\boldsymbol{\alpha}}_1$. The CLF is proposed as

$$\mathbf{V}_2 = \mathbf{V}_1 + \frac{1}{2}\mathbf{z}_2^T\mathbf{M}\mathbf{z}_2 + \frac{1}{2}\tilde{\boldsymbol{\zeta}}^T\mathbf{K}_i\tilde{\boldsymbol{\zeta}}. \tag{22}$$

Differentiating $\mathbf{V}_2$ and inserting for $\dot{\mathbf{V}}_1$, $\dot{\mathbf{z}}_2$, and $\dot{\tilde{\boldsymbol{\zeta}}}$ gives

$$\begin{aligned}\dot{\mathbf{V}}_2 = &-\mathbf{z}_1^T\mathbf{Q}_1\mathbf{z}_1 + \mathbf{z}_1^T\mathbf{z}_2 + \mathbf{z}_2^T[-\mathbf{D}_L\mathbf{z}_2 - \mathbf{D}_L\boldsymbol{\alpha}_1 \\ &+ \boldsymbol{R}^T(\psi)\mathbf{b} + \mathbf{u} - \mathbf{M}\dot{\boldsymbol{\alpha}}_1 + \mathbf{K}_i\tilde{\boldsymbol{\zeta}}].\end{aligned}$$

$\dot{\boldsymbol{\alpha}}_1$ is calculated in Eqn. (21). The control input $\mathbf{u}$ is chosen as

$$\mathbf{u} = \mathbf{D}_L\boldsymbol{\alpha}_1 - \mathbf{z}_1 + \mathbf{M}\dot{\boldsymbol{\alpha}}_1 - \mathbf{R}^T(\psi)\mathbf{K}_i\boldsymbol{\zeta} - \mathbf{Q}_2\mathbf{z}_2, \tag{23}$$

where $\mathbf{Q}_2 = \mathbf{Q}_2^T > \mathbf{0}$. The part of $\dot{\mathbf{V}}_2$ $\mathbf{R}^T(\psi)(\mathbf{b} - \mathbf{K}_i\boldsymbol{\zeta}) - \mathbf{K}_i\tilde{\boldsymbol{\zeta}}$ cancels due to the definition of $\tilde{\boldsymbol{\zeta}}$, which leaves

$$\dot{\mathbf{V}}_2 = -\mathbf{z}_1^T\mathbf{Q}_1\mathbf{z}_1 - \mathbf{z}_2^T(\mathbf{D}_L + \mathbf{Q}_2)\mathbf{z}_2, \tag{24}$$

where $(\mathbf{D}_L + \mathbf{Q}_2) > 1$. The closed-loop system is

$$\dot{\mathbf{z}}_1 = -\mathbf{Q}_1\mathbf{z}_1 + \mathbf{z}_2, \tag{25a}$$

$$\dot{\tilde{\boldsymbol{\zeta}}} = \mathbf{z}_2 \tag{25b}$$

$$\dot{\mathbf{z}}_2 = \mathbf{M}^{-1}[-\mathbf{z}_1 - \mathbf{K}_i\tilde{\boldsymbol{\zeta}} - (\mathbf{D}_L + \mathbf{Q}_2)\mathbf{z}_2] \tag{25c}$$

**Proposition A1** The equilibrium $(\mathbf{z}_1, \tilde{\boldsymbol{\zeta}}, \mathbf{z}_2) = (\mathbf{0},\mathbf{0},\mathbf{0})$ of the closed-loop system Eqn. (25) with $\mathbf{b} \neq \mathbf{0}$ uniformly globally asymptotically stable (UGAS). Then $\boldsymbol{\zeta} = \mathbf{K}_i^{-1}\mathbf{b}$.

**Sketch of Proof** By applying an invariance-like theorem for time varying systems, for example Matrosov's theorem [18, Theorem 1], the origin of Eqn. (25) can be proven (UGAS). Eqn. (24) is negative semi definite and yields $(\mathbf{z}_1, \tilde{\boldsymbol{\zeta}}, \mathbf{z}_2) = (\mathbf{0},\mathbf{0},\mathbf{0})$ uniformly globally stable (UGS). Define $\mathbf{W}_1 := \mathbf{V}_2$ and $\mathbf{W}_2 := \tilde{\boldsymbol{\zeta}}^T\mathbf{M}\mathbf{z}_2$, and also $\mathbf{Y}_1 := -\mathbf{z}_1^T\mathbf{Q}_1\mathbf{z}_1 - \mathbf{z}_2^T(\mathbf{D}_L + \mathbf{Q}_2)\mathbf{z}_2$ and $\mathbf{Y}_2 := \mathbf{z}_2^T\mathbf{z}_2 + \tilde{\boldsymbol{\zeta}}^T[-\mathbf{z}_1 - \mathbf{K}_i\tilde{\boldsymbol{\zeta}} - (\mathbf{D}_L + \mathbf{Q}_2)\mathbf{z}_2]$. Then $\dot{\mathbf{W}}_1 = \mathbf{Y}_1$ and $\dot{\mathbf{W}}_2 = \mathbf{Y}_2$. The time-varying part of $\mathbf{Y}_i, i = 1,2$ lies in $\boldsymbol{\eta}^*(t), \dot{\boldsymbol{\eta}}^*(t)$ which are continuous and bounded. Choose $\boldsymbol{\phi}(t,x) = \boldsymbol{\eta}^*(t)$, then $\mathbf{Y}_i = \mathbf{Y}_i(\mathbf{z}_1, \tilde{\boldsymbol{\zeta}}, \mathbf{z}_2, \boldsymbol{\phi}), i = 1,2$. $\boldsymbol{\phi}(t,x)$ and $\mathbf{W}_1, \mathbf{W}_2$ are bounded for bounded $(\mathbf{z}_1, \tilde{\boldsymbol{\zeta}}, \mathbf{z}_2)$. If $\tilde{\boldsymbol{\zeta}} = \mathbf{0}$, then $\mathbf{Y}_1 = \mathbf{0} \rightarrow \mathbf{Y}_2 \leq \mathbf{0}$, and $\mathbf{Y}_1 = \mathbf{Y}_2 = \mathbf{0} \rightarrow (\mathbf{z}_1, \tilde{\boldsymbol{\zeta}}, \mathbf{z}_2) = (\mathbf{0},\mathbf{0},\mathbf{0})$.

**Resulting Control Law** In this application the desired state is constant; $\dot{\boldsymbol{\eta}}^* = \ddot{\boldsymbol{\eta}}^* = \mathbf{0}$, and $r$ and $\dot{r}$ are small ($\approx 0$). Rewriting Eqn. (23) in the original states and simplifying gives the nonlinear PID control law Eqn. (6), with $\mathbf{K}_a = \mathbf{0}$.

## Appendix B: Well-posedness

(A1) $C$ and $D$ are closed subsets of $\mathbb{R}^n$

(A2) The flow map is a continuous function on a closed set, so it is OSC and convex. It is also locally bounded, and $C \subset \text{dom } F$.

(A3) The jump map contains continuous function on closed intervals and the spectral analysis function $\Upsilon$. $\Upsilon$ is based on DFT formulas, and is therefore continuous. The set-valued mapping

$$\chi \mapsto \arg\min_{\alpha \in Q} |\Upsilon(\chi) - \omega_{p,\alpha}|$$

has the same structure as the mapping $M(x)$ in Example 5.11 [1]. $\alpha$ plays the role of $y$, $Q$ plays the role of $K$, $\chi$ plays the role of $x$, and $|\Upsilon(\chi) - \omega_{p,\alpha}|$ plays the role of $\phi(x,y)$. $M(x)$ is OSC, so therefore the jump map is OSC. It is also bounded with $D \subset \text{dom } G$.

(A1)-(A3) are satisfied, so the hybrid system $\mathscr{H}$ is well-posed.

# Paper 2

# Sensor-Based Hybrid Observer for Dynamically Positioned Vessels

Astrid H. Brodtkorb, Andrew R. Teel, Asgeir J. Sørensen

Submitted to the *2014 IEEE Multi-conference on Systems and Control, (MSC)*.

# Sensor-Based Hybrid Observer for Dynamically Positioned Vessels*

Astrid H. Brodtkorb[1], Andrew R. Teel[2] and Asgeir J. Sørensen[1]

*Abstract*— **Observers are important components of dynamic positioning (DP) systems, estimating unmeasured states and bias, filtering out waves, and predicting states in the case of signal loss. In this paper, a simplified sensor-based hybrid observer concept is investigated. The concept assumes that acceleration measurements are readily available, and can be integrated to obtain position estimates. Position measurements are taken occasionally, and at these instances the position estimate is updated. Major contributions of this paper include the design, stability analysis and simulation of two one degree of freedom (1DOF) sensor-based hybrid observers which rely on acceleration, velocity and position measurements.**

## I. INTRODUCTION

The fleet of dynamically positioned (DP) ships and rigs is growing due to offshore oil and gas operations moving farther from shore, into deeper waters and harsher environments. High day rates and strict requirements securing safety motivates highly reliable and environmentally friendly DP system solutions.

In many DP controllers today a model-based estimator is included in the controller structure, for example an extended Kalman filter [1], [2], or a nonlinear passive observer [3]. The observer uses noisy GPS, hydro-acoustic, laser or microwave measurements to reconstruct unmeasured states, filter out wave frequency motions, estimate bias, and in case of signal loss do dead reckoning. The bias estimate contains the slowly varying forces acting on the vessel, unmodeled dynamics and transient behavior in for example start-up. In case of rapid changing disturbances, the bias estimate is a weakness of the model-based observer.

Another observer type is based on measurements only, and is often called a sensor-based observer, or strap-down approach. [4] presents a nonlinear method for estimating linear and angular velocity of accelerated vehicles, and [5], [6] propose an observer which integrates acceleration measurements from the inertial measurement unit (IMU) to obtain position estimates. These are corrected with position measurements from for example GPS or High Precision Positioning (HiPAP) systems. Accelerometer bias and drifting may cause large deviations in the position estimates due to the integration [7].

The position, velocity and acceleration measurements of a vessel in DP are taken at different sampling rates, and can be incorporated into a *measurement model*. The hybrid dynamical systems framework proposed in [8] allows the integration of change on different time scales into one system. The work presents a mathematical framework, which can be applied to a wide range of systems, and discusses stability and robustness for these. The mathematical model consists of a continuous part which evolves by *flowing*, and a discrete part which changes in *jumps*.

The major contributions of this paper include the design of two sensor-based observers using the framework of hybrid dynamical systems described in [8] applied to a process motivated by the measurements obtained on a vessel in DP. For simplification, the process is assumed to have continuous acceleration measurements and occasional position and velocity measurements. This is modeled as a hybrid system where the acceleration measurements are integrated to obtain position and velocity estimates in the flow map, and the updates with occasional position and velocity measurements are in the jump map.

Two observers are designed using this approach, both accounting for measurement noise by averaging $N$ past measurements. The first observer is a special case of the second observer. Stability is analyzed for both observers using stability results for sets, providing uniform global asymptotic stability (UGAS). The first observer is reproven UGAS with Lyapunov analysis in order to facilitate the stability analysis in the future work, involving systems with randomness. The two observers are implemented in one degree of freedom (1DOF) and simulated using Matlab/Simulink. The simulation results are compared.

The paper is organized as follows: In Section II the hybrid measurement model is derived based on a simplified model of a vessel in DP. In Section III the two observers are designed, and in Section IV stability is argued. In Section V simulation results from Matlab/Simulink are presented and discussed, and Section VI concludes the paper.

## II. MATHEMATICAL MODELING

This section briefly introduces the hybrid framework and modeling of a marine vessel in DP, before the hybrid measurement model is established.

### A. Hybrid Dynamical Systems Framework

The hybrid dynamical systems framework presented in [8] can be used to describe systems with both continuous (flows)

*This work was supported by the Research Council of Norway through the Centres of Excellence funding scheme, project number 223254 AMOS, and in part by AFOSR grant FA9550-12-1-0127, and NSF grant ECCS-1232035.

[1]Centre for Autonomous Marine Operations (AMOS), Department of Marine Technology, Norwegian University of Science and Technology (NTNU), Otto Nielsens vei 10, 7491 Trondheim, Norway, astrid.h.brodtkorb@ntnu.no, asgeir.sorensen@ntnu.no

[2] Center for Control, Dynamical Systems, and Computation, Department of Electrical Engineering, University of California, Santa Barbara, CA 93106-9560 teel@ece.ucsb.edu

Preprint submitted to 2014 IEEE Multi-conference on Systems and Control.
Received April 10, 2014.

and instantaneous (jumps) change. In general the system can be modeled as

$$x \in C \quad \dot{x} \in F(x), \tag{1a}$$
$$x \in D \quad x^+ \in G(x), \tag{1b}$$

where $C$ is the flow set, $F$ is the flow map, $D$ is the jump set, and $G$ is the jump map. If a system can be written as in (1) and is well-posed,[1] the stability and robustness results from [8] can be applied to check the stability properties of the system.

### B. Marine Vessel Modeling

Two nonlinear second-order models of different complexities are used to describe a marine vessel in waves, wind and current. The process plant model is a high fidelity model in 6DOF describing the vessel response as accurately as needed, and is used for numerical testing of controllers. A simplified model called a control plant model contains only the most important dynamics, and is in 3DOF for a surface vessel. Model-based controllers and observers, and Lyapunov stability analysis are based on the control plant model. See [10] and [11] for modeling details.

Sensors on board the vessel usually provide noisy position, velocity and acceleration measurements which are sampled at different rates. The noise is assumed to follow a zero mean Gaussian distribution.

### C. Hybrid Measurement Model

Motivated by a ship in DP, a measurement model including acceleration, velocity and position measurements is proposed. The position measurement $\xi$ and velocity measurement $v$ are assumed to be taken occasionally, not necessarily periodically, triggered by a counter variable $\tau \in [0, T_{max}]$. The maximum sample time between the $(\xi, v)$-measurements is $T_{max}$, and the minimum sample time is $T_{min} > 0$.

The acceleration measurements $\dot{v} \in Z$ are assumed to be taken continuously, so $\dot{v}$ integrated to obtain velocity $v$ and position $\xi$ can be represented as the measurement flow dynamics

$$(\xi, v) \in K \quad \begin{cases} \dot{\xi} = v, \\ \dot{v} \in Z. \end{cases} \tag{2}$$

$K \subset \mathbb{R}^{2m}$ and $Z \subset \mathbb{R}^m$ are assumed compact. Compactness of $K$ forces $(\xi, v)$ to be bounded, which is physically realistic. $Z$ is also assumed convex. Throughout this paper, the measured acceleration $\dot{v}$ is assumed to be equal to the real acceleration of the vessel, i.e. the acceleration sensor is ideal giving no noise or bias on the measurements. In reality IMU measurements contain noise and bias, and are prone to drifting. Integrating noise or bias cause large errors in position estimation, which may destabilize the system. However, this is not a topic covered in this paper.

[1] Well-posedness is guaranteed by the data $(C, F, D, G)$ satisfying regularity properties; see [8, Theorem 6.30]. These regularity properties include $C$ and $D$ being closed; if $F$ and $G$ are functions defined on $C$ and $D$, respectively, then they should be continuous; here $F$ and $G$ are set-valued mappings, which are a more general than functions. In that case, they should have closed graphs, be locally bounded, and should be nonempty on $C$ and $D$, respectively; moreover, the values $F(x)$ should be convex for each $x \in C$. See also (A1)-(A3) in Section IV.

## III. HYBRID OBSERVER DESIGN

In this section two observers are designed for position estimation. The general principle for the observers is for the states to flow according to (2) with the available acceleration measurement $\dot{v}$, denoted $a$, and update the observer states with the occasional measurement $(\xi, v)$. The flows act as the predictor, and the jumps act like the corrector. Both observers store $N$ of the past measurements, and compute an estimate $(\hat{\xi}, \hat{v})$ by averaging the observer states. Observer 1 is a special case of observer 2. The observer states are denoted $(\xi_i, v_i)\ i \in \{1, ..., N\}$ where $(\xi_1, v_1)$ are the most recent measurements and $(\xi_N, v_N)$ are the least recent measurements. Table I gives an overview of the notation.

| Notation | Description |
|---|---|
| $(\xi, v, a) \in K \times Z$ | Measurements; position, velocity, acceleration |
| $(\xi_i, v_i) \in \mathbb{R}^{2m}$ | Observer states; position, velocity |
| $(\hat{\xi}, \hat{v}) \in \mathbb{R}^{2m}$ | Observer estimates; position, velocity |

TABLE I
NOTATION

### A. Observer 1

The flow dynamics for the observer states $(\xi_i, v_i),\ i \in [1, ..., N]$ is a copy of (2),

$$(\xi_i, v_i) \in \mathbb{R}^{2m}, \ \begin{cases} \dot{\xi}_i = v_i, \\ \dot{v}_i = a, \end{cases} \tag{3a}$$
$$\tau \in [0, T_{max}], \quad \dot{\tau} = -1, \tag{3b}$$

The observer states flow with the acceleration measurement $a$ in between the updates when $\tau \in [0, T_{max}]$. The jump dynamics is

$$(\xi, v) \in K, \quad \xi_1^+ = \xi, \quad v_1^+ = v, \tag{4a}$$
$$(\xi_i, v_i) \in \mathbb{R}^{2m}, \quad \xi_i^+ = \xi_{i-1},\ v_i^+ = v_{i-1},\ i \in \{2, .., N\} \tag{4b}$$
$$\tau = \{0\},\ \tau^+ \in [T_{min}, T_{max}]. \tag{4c}$$

The variables $(\xi_1, v_1)$ load in the most recent measurements in (4a), and the states are shifted one place back in (4b). The update is triggered when $\tau = \{0\}$. $\tau$ is reset in the interval $[T_{min}, T_{max}]$ to ensure at least $T_{min}$ seconds between each update and at most $T_{max}$ seconds. The observer estimates are:

$$\hat{\xi} = \frac{1}{N} \sum_{i=1}^{N} \xi_i, \quad \hat{v} = \frac{1}{N} \sum_{i=1}^{N} v_i,$$

### B. Observer 2

For observer 2, the same concept as observer 1 is applied, but now the average is computed in the intermediate processing as well. Observer 2 uses the states $(\xi_i, v_i),\ i \in \{1, .., N\}$,

Preprint submitted to 2014 IEEE Multi-conference on Systems and Control.
Received April 10, 2014.

and the flow dynamics is

$$(\xi_i, v_i) \in \mathbb{R}^{2m}, \ \begin{cases} \dot{\xi}_i = \frac{1}{N}\sum_{j=1}^{N} v_j, \\ \dot{v}_i = a, \end{cases} \tag{5a}$$

$$\tau \in [0, T_{max}], \quad \dot{\tau} = -1, \tag{5b}$$

and the jump dynamics

$$(\xi, v) \in K, \quad \begin{cases} \xi_1^+ = \xi, \\ v_1^+ = v \end{cases} \tag{6a}$$

$$(\xi_i, v_i) \in \mathbb{R}^{2m}, \quad \begin{cases} \xi_i^+ = \xi_{i-1}, \\ v_i^+ = v_{i-1}, \end{cases} \quad i \in \{2, .., N\} \tag{6b}$$

$$\tau = \{0\}, \ \tau^+ \in [T_{min}, T_{max}]. \tag{6c}$$

The difference between the observers shows in (5a) where the position state is updated with the average of the velocity states. The estimates for $\xi$ and $v$ for observer 2 are

$$\hat{\xi} = \frac{1}{N}\sum_{i=1}^{N} \xi_i, \ \hat{v} = \frac{1}{N}\sum_{i=1}^{N} v_i.$$

## IV. STABILITY ANALYSIS

For hybrid systems, stability of a set should be evaluated. Stability results from [8] used in this section are stated, before stability of the observers is discussed. First stability based on set invariance and convergence is proven, and for the sake of future work Lyapunov analysis for observer 1 is also included.

### A. Stability Results

*Stability Based on Set Invariance and Convergence*

This stability analysis uses the notions of *strong forward invariance* and *uniform attractivity*. If for every maximal solution $\phi$ starting in $\mathcal{A}$, the range of $\phi$ is in a subset of $\mathcal{A}$, then $\mathcal{A}$ is strongly forward pre-invariant[2], [8, Def. 6.25]. A compact set $\mathcal{A} \subset \mathbb{R}^n$ is said to be uniformly pre-attractive from a set $S \subset \mathbb{R}^n$ if every $\phi \in \mathcal{S}_{\mathcal{H}}(S)$ is bounded and for every $\epsilon > 0$ there exists a $T > 0$ such that $|\phi(t,j)|_{\mathcal{A}} \leq \epsilon$ for every $\phi \in \mathcal{S}_{\mathcal{H}}(S)$ and $(t,j) \in$ dom $\phi$ with $t + j \geq T$, [8, Def. 6.24].

*Proposition 1 [8, Def. 7.3 and Prop. 7.5] Stability from invariance plus uniform convergence*
(a) Let the hybrid system $\mathcal{H}$ be nominally well-posed.
(b) Suppose that a compact set $\mathcal{A} \subset \mathbb{R}^n$ has the following properties:

i. it is strongly forward invariant, and
ii. is it uniformly attractive from a neighborhood of itself, i.e. there exists a $\mu > 0$ such that $\mathcal{A}$ is uniformly attractive from $\mathcal{A} + \mu\mathbb{B}$
iii. the basin of attraction of $\mathcal{A}$, denoted $\mathcal{B}_{\mathcal{A}}^p$, is all of $\mathbb{R}^n$. $\mathcal{B}_{\mathcal{A}}^p$ is the set of points $\xi \in \mathbb{R}^n$ such that every solution $\phi$ to $\mathcal{H}$ with $\phi(0,0) = \xi$ is bounded, and if it is complete, then also $\lim_{t+j\to\infty} |\phi(t,j)|_{\mathcal{A}} = 0$.

Then the compact set $\mathcal{A}$ is UGAS. □

[2]The *pre-* allows for the possibility that maximal solutions are not complete.

Nominal well-posedness is satisfied if the hybrid system satisfies the hybrid basic conditions [8, Assumption 6.5] . These are:

(A1) $C$ and $D$ are closed subsets of $\mathbb{R}^n$;
(A2) The set-valued mapping $F : \mathbb{R}^n \rightrightarrows \mathbb{R}^n$ is outer semi-continuous[3] (OSC) and locally bounded relative to $C$, $C \subset$ dom $F$, and $F(x)$ is convex for every $x \in C$;
(A3) The set-valued mapping $G : \mathbb{R}^n \rightrightarrows \mathbb{R}^n$ is OSC and locally bounded relative to $D$, and $D \subset$ dom $G$.

*Lyapunov-based Stability Analysis*

Lyapunov functions can be used to analyze stability of hybrid systems. A Lyapunov function candidate is defined in Definition 1, and conditions for stability are stated in Theorem 1.

*Definition 1 [8, Def. 3.16] Lyapunov function candidate*
A function $V$ : dom $V \to \mathbb{R}^n$ is said to be a Lyapunov function candidate for the hybrid system $\mathcal{H} = (C, F, D, G)$ if the following conditions hold:

1. $\bar{C} \cup D \cup G(D) \subset$ dom $V$,
2. $V$ is continuously differentiable on an open set containing $\bar{C}$,

where $\bar{C}$ denotes the closure of $C$. □

*Theorem 1 [8, Thm. 3.18 ] Sufficient Lyapunov conditions*
Let $\mathcal{H} = (C, F, D, G)$ be a hybrid system and let $\mathcal{A} \subset \mathbb{R}^n$ be closed. If $V$ is a Lyapunov function candidate for $\mathcal{H}$, and there exists $\alpha_1, \alpha_2 \in K_\infty$, and a continuous positive definite function $\rho$ such that

i) $\alpha_1(|x|_{\mathcal{A}}) \leq V(x) \leq \alpha_2(|x|_{\mathcal{A}}) \quad \forall x \in C \cup D \cup G(D)$
ii) $< \nabla V(x), f > \leq -\rho(|x|_{\mathcal{A}}) \quad \forall x \in C, f \in F(x)$
iii) $V(g) - V(x) \leq -\rho(|x|_{\mathcal{A}}) \quad \forall x \in D, g \in G(x)$

then $\mathcal{A}$ is UGAS for $\mathcal{H}$. □

Sufficient conditions for ii) and iii) are

ii*) $< \nabla V(x), f > \leq -\epsilon V(x) \quad \forall x \in C, f \in F(x)$,
iii*) $V(g) = (1-\epsilon)V(x) \quad \forall x \in D, g \in G(x)$,

with $\epsilon > 0$.

### B. Stability Based on Set Invariance and Convergence

The set for both observers is

$$\begin{aligned} \mathcal{A} := \{&(\xi, v, \xi_1, v_1, ..., \xi_N, v_N, \tau) : \\ &(\xi, v) \in K, \xi = \xi_1 = ... = \xi_N, v = v_1 = ... = v_N, \\ &\tau \in [0, T_{max}]\}, \end{aligned} \tag{7}$$

which are values the states take when they have converged to the measurement. $\tau \in [0, T_{max}]$ is always satisfied.

[3]A set-valued mapping $H : \mathbb{R}^n \rightrightarrows \mathbb{R}^n$ is OSC if for each convergent sequence $\{(x_i, y_i)\}_{i=1}^{\infty}$ that satisfies $y_i \in H(x_i), \forall i \geq 1$ and the limit denoted $(x, y)$ satisfies $y \in H(x)$. If $F : C \to \mathbb{R}^n$ is continuous and $C$ is closed, then $F$ is OSC.

Preprint submitted to 2014 IEEE Multi-conference on Systems and Control.
Received April 10, 2014.

*Stability Analysis of Observer 1*

(a) Observer 1 given by (3)-(4) can be shown well-posed by satisfying the hybrid basic conditions:

(A1) The set $K$ is assumed to be compact. Compact implies that a set is closed and bounded. $[0, T_{max}]$ is a closed interval, and the point $\{0\}$ is a special case of a closed set. This implies that $C$ and $D$ are closed subsets of $\mathbb{R}^n$.

(A2) Since the flow dynamics (3) is continuous and $K \times [0, T_{max}]$ is closed, the flow map is OSC. The flow map is nonempty because it is defined for each $(\xi_i, v_i, \tau) \in C$.

(A3) The jump dynamics (4) is a continuous function on a closed set $K \times \{0\}$, so it is OSC. It is also nonempty because it is defined for each $(\xi_i, v_i, \tau) \in D$.

(b) $\mathcal{A}$ is a subset of $C$ where $\xi_i = \xi, v_i = v \ \forall i$, which is both closed and bounded. $[0, T_{max}]$ is a closed interval, so $\mathcal{A}$ is compact.

i. If the initial condition is within the set $\mathcal{A}$, it is given that during flows $(\xi_i, v_i), \forall i$ will stay in $\mathcal{A}$. At jumps the most recent position and velocity measurements $(\xi, v)$ are saved to the states $(\xi_1, v_1)$. The stored estimates $(\xi_1, v_1)$ are shifted to $(\xi_2, v_2)$, $(\xi_2, v_2)$ are shifted to $(\xi_3, v_3)$, and so on. When starting in $\mathcal{A}$, $(\xi, v) = (\xi_1, v_1) = (\xi_2, v_2) = ... = (\xi_N, v_N)$ is always satisfied. The timer $\tau$ is constrained to the interval $[0, T_{max}]$ for both flows and jumps.

ii. If the starting value is $(\xi_1, v_1)$, it becomes $(\xi, v)$ after one jump. Starting at $(\xi_2, v_2)$, after one jump it will be $(\xi_1, v_1)$, and after two jumps it will converge to $(\xi, v)$. So then, if the starting value is $(\xi_\mu, v_\mu)$ then after $\mu$ jumps $\mathcal{A}$ is reached. The set is reached in at most N jumps, so $\mathcal{A}$ is uniformly attractive from a neighborhood of itself.

iii. All initial values for $(\xi_i, v_i, \tau) \in \mathbb{R}^{2n} \times [0, T_{max}]$ satisfy point ii. This means that the basin of attraction $\mathcal{B}^p_{\mathcal{A}}$ is the whole space $\mathbb{R}^n$, and $\mathcal{A}$ is uniformly attractive from $\mathbb{R}^n$.

It follows from Proposition 1 that the set $\mathcal{A}$ is UGAS for observer 1.

*Stability of Observer 2*

a) Observer 2 given by (5)-(6) is well-posed. This is because during flows convex combinations, the average, of already closed and bounded $v_i$ are computed for each $\xi_i$. The flow set, jump map and jump set are unchanged.

b) $\mathcal{A}$ is compact, see the previous section.

i. When starting in $\mathcal{A}$, the average of $v_i$ is within $\mathcal{A}$, and so flows stay within the set. The updates at jumps are the same as for observer 1; the most recent measurement is stored in $(\xi_1, v_1)$, and the states are shifted one place back. When starting in $\mathcal{A}$, $(\xi, v) = (\xi_1, v_1) = (\xi_2, v_2) = ... = (\xi_N, v_N)$ is always satisfied, and $\mathcal{A}$ is strongly forward invariant for observer 2 as well.

ii. Looking at (6b), and starting with $v_N$. After one jump $v_N$ agrees with $v_{N-1}$, and after $N$ jumps $v_N$ agrees with $v_1$. After one jump $v_1$ agrees with $v$ which is estimated as $\frac{1}{N}\sum_{i=1}^{N} v_i$. This means that $\frac{1}{N}\sum_{i=1}^{N} v_i$ agrees with $v$ after $N$ jumps. During flows, (5a), $\xi_1$ agrees with $\xi$ after $N+1$ jumps, and $\xi_N$ agrees with $\xi$ after $2N$ jumps. $\mathcal{A}$ is reached in at most $2N$ jumps, which means that the set is uniformly attractive from a neighborhood of itself.

iii. Regardless of which values the initial conditions have, point ii. is satisfied in at most $2N$ jumps. Then the basin of attraction $\mathcal{B}^p_{\mathcal{A}_2}$ is $\mathbb{R}^n$, and $\mathcal{A}$ is uniformly attractive from the whole space $\mathbb{R}^n$.

It follows from Proposition 1 that the set $\mathcal{A}$ is UGAS for observer 2.

*Lyapunov Analysis*

Proposition 1 is straight forward and concludes UGAS of both observers. This section reproves this result for observer 1 using Lyapunov analysis. The analysis is a step towards using Lyapunov analysis tools in [12] to establish certain recurrence properties for systems with random noise.

The Lyapunov conditions for a well-posed hybrid system are stated in Theorem 1, Section IV-A. For convenience, (3) and (4) are rewritten in terms of error flow dynamics

$$(\xi, v) \in K \quad \dot{e}_i = Ae_i, \ \forall i \in \{1, .., N\}, \tag{8a}$$

$$\tau \in [0, T_{max}] \quad \dot{\tau} = -1, \tag{8b}$$

and error jump dynamics

$$(\xi, v) \in K \quad e_1^+ = 0, \quad e_i^+ = e_{i-1} \quad \forall i \in \{2, .., N\} \tag{9a}$$

$$\tau = \{0\} \quad \tau^+ \in [T_{min}, T_{max}]. \tag{9b}$$

where

$$\zeta_0 := (\xi, v)^T, \ \zeta_i := (\xi_i, v_i)^T, \ e_i := \zeta_i - \zeta_{i-1}, \ \forall i \in \{1, .., N\}$$

and

$$A := \begin{bmatrix} 0 & 1 \\ 0 & 0 \end{bmatrix}.$$

Then the set $\mathcal{A}$ corresponds to when $e_i = 0 \ i \in \{1, ..., N\}, \ \tau \in [0, T_{max}]$, which is more favorable for Lyapunov analysis. Further, let $P = P^T > 0$ and $\mu > 0$ be such that:

$$A^T P + PA \leq \mu P, \tag{10}$$

and $\lambda > \mu$. Define $c_{N+1} = 0$ and $c_i > 0, i \in \{1, .., N\}$ satisfying

$$\frac{c_{i+1}}{c_i} < \exp(-\lambda T_{max}) \quad \forall i \in \{1, .., N\}. \tag{11}$$

The proposed Lyapunov function candidate is

$$V(x) = \exp(\lambda \tau) \sum_{i=1}^{N} c_i e_i^T P e_i \tag{12}$$

where $x = [e_i, \tau]^T$. $V : \mathbb{R}^n \to \mathbb{R}_{\geq 0}$ is a Lyapunov function candidate for (8) and (9) because it satisfies Definition 1. $V(x) = 0$ if and only if $e_i = 0$, which is the case only when $x$ has converged to the set $\mathcal{A}_1$. Applying Theorem 1 to (8) and (9):

Preprint submitted to 2014 IEEE Multi-conference on Systems and Control.
Received April 10, 2014.

i) Choosing the smallest value of $\tau = T_{min}$ and the largest value of $\tau = T_{max}$ gives lower and upper bounds on $V(x)$.

ii*)

$$< \nabla V(x), f > = \exp(\lambda\tau) \sum_{i=1}^{N} \left(-\lambda c_i e_i^T P e_i + c_i 2 P \dot{e}_i\right)$$

Using that $\dot{e}_i = Ae_i$, and $A^T P + PA \leq \mu P$ gives

$$< \nabla V(x), f > \leq -\lambda V(x) + \mu V(x) \leq -\epsilon V(x),$$

with $\epsilon = \lambda - \mu > 0$.

iii*)

$$V(g) \leq \exp(\lambda T_{max}) \sum_{i=2}^{N} c_i e_{i-1}^T P e_{i-1}$$
$$= \exp(\lambda T_{max}) \sum_{i=1}^{N-1} c_{i+1} e_i^T P e_i$$

Using (11) and simplifying gives

$$V(g) \leq \exp(\lambda T_{max}) \sum_{i=1}^{N} \frac{c_{i+1}}{c_i} c_i e_i^T P e_i$$
$$= \exp(\lambda T_{max}) \sum_{i=1}^{N} \left(\frac{c_{i+1}}{c_i}\right) V(x)$$
$$\leq \exp(\lambda T_{max}) \max_{i \in \{1,\ldots,N\}} \left(\frac{c_{i+1}}{c_i}\right) V(x)$$
$$\leq (1-\epsilon) V(x)$$

By Theorem 1, the set $\mathcal{A}$ is UGAS for observer 1.

## V. SIMULATION RESULTS AND DISCUSSION

This section presents the simulation setup and discusses the results. Simulations are done for $m = 1$, 1DOF, and neglecting the rotation between reference frames, see [11] for details on marine vessel modeling.

### A. Setup

Both observers are implemented into Matlab/Simulink using the hybrid simulation toolbox described in [13]. The measurements $(\xi, v, a)$ are generated using a reference model, see [7] for details, with noise added on $(\xi, v)$ in stead of simulating a process plant model, controller and observer in closed loop. This approximation gives a good indication of the potential observer performance. However, the behavior of the observer in closed loop with an output feedback controller may be different than the results obtained here indicate.

### B. Results and Discussion

The simulation results presented have $N = 5$ number of states in the observer, and the initial conditions $x_{i0} := (\xi_i(0), v_i(0)), \forall i = \{1, ..., N\}$ are equal to the initial measurement $x_0 := (\xi(0), v(0))$, and $\tau(0) = 1$. $\tau \in [T_{min}, T_{max}] = [1, 10]$. Two cases are simulated, one where the vessel has constant setpoint, see Figs. 1 and 2,

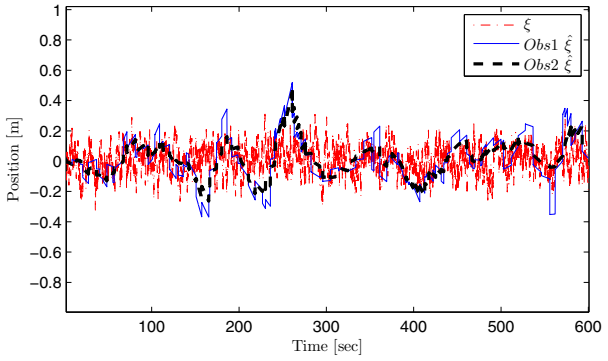


Fig. 1. Observer performance, setpoint unchanged. $N = 5$, $\tau \in [1, 10]$, $x_{i0} = x_0$

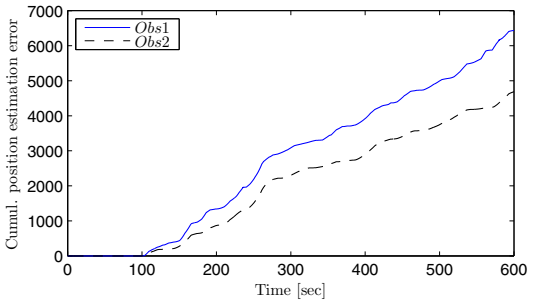


Fig. 2. Cumulative estimation error, setpoint unchanged. $N = 5$, $\tau \in [1, 10]$, $x_{i0} = x_0$

and one where the setpoint changes, see Figs. 3 and 4. Observer 2 has best performance in the presented simulation scenarios, however the performance is highly dependent on $N, [T_{min}, T_{max}]$ and $x_{i0}$. A parameter study follows for the case when the setpoint is constant at zero, see Table II for cumulative position estimation error (CPEE) at $t = 600$ seconds. The first $2NT_{max}$ seconds of the simulation is neglected when computing the CPEE, so both observers have reached steady state. The exception is when the effect of initial conditions is investigated, see the last study in Table II. The error is also calculated based on the ideal, nonnoisy, $(\xi, v)$. The CPEE is somewhat larger for when the setpoint changes, but follows the same trends.

The first study in Table II show that when $N = 1$ the observers are identical and have the exact same performance. When $N$ increases, and $\tau \in [1, 20]$, observer 1 has steadily decreasing performance. Observer 2 has decreasing performance at first, and then increasing performance after $N = 7$.

The second study in Table II investigates the sensitivity of the observers to the update time $T_{max}$. As expected, updating the states more frequently improves both observers' performance significantly. When $N = 5$ and $x_{i0} = x_0$ observer 2 is a bit more sensitive to $T_{max}$ than what observer 1 is. CPEE for observer 2 is reduced by 66.3% and for observer 1 by 64.1% when $T_{max}$ changes from 20 to 3.

The last study in Table II shows the transient observer behavior and the importance of correct initialization. The first

Preprint submitted to 2014 IEEE Multi-conference on Systems and Control.
Received April 10, 2014.

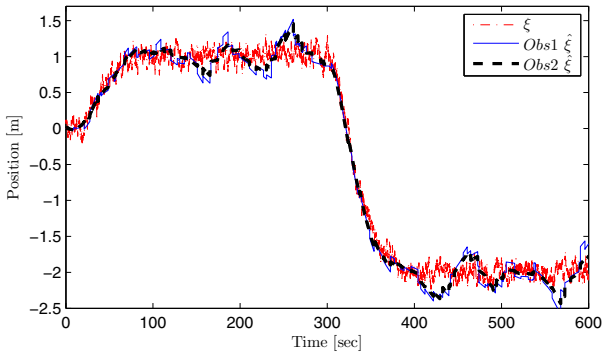


Fig. 3. Observer performance, setpoint changed. $N = 5$, $\tau \in [1, 10]$, $x_{i0} = x_0$

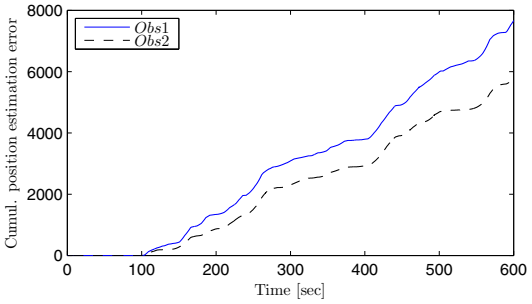


Fig. 4. Cumulative estimation error, setpoint changed. $N = 5$, $\tau \in [1, 10]$, $x_{i0} = x_0$

column with $N = 10$ and $x_{i0} = x_0$ is the same simulation as the first study, last column when $N = 10$, only with and without the transients included in the CPEE calculation. For wrong initialization, $x_{i0} \neq x_0$, and $N = 1$ the performance of the observers is not affected very much. However, with increasing $N$ the correct initialization is more important, especially for observer 2, which is slower to reach steady state.

Nonnoisy acceleration measurements $a$ were assumed. Simulations show that both observers are robust to acceleration noise, although performance is affected negatively. The observers showed no sensitivity to varying noise amplitude in the measurements $(\xi, v, a)$.

## VI. CONCLUSION

The observers' performance is highly dependent on the number of states $N$ in the observer, the initializing of the states, and the maximum update time $T_{max}$. Observer 2 performs better for large $N$, and observer 1 performs better for small update intervals. Initializing the observers correctly is of increasing importance when $N$ increases.

For further work, simulations with a process plant model, controller and observer should be done to ensure that the closed loop system is well behaved. The Lyapunov analysis in Section IV should be extended to establish certain *recurrence* properties for systems with randomness by applying Lyapunov analysis tools developed in [12]. Both observers should also be simulated in 3DOF including body rotations, so estimation for a surface vessel in DP can be achieved.

$N$-dependence when $\tau \in [1, 20]$, $x_{i0} = x_0$

| CPEE | $N = 1$ | $N = 4$ | $N = 5$ | $N = 10$ |
|---|---|---|---|---|
| Obs 1 | 8574 | 11110 | 11710 | 11750 |
| Obs 2 | 8574 | 10120 | 10850 | 8597 |

$T_{max}$-dependence when $N = 5$, $x_{i0} = x_0$

| CPEE | $\tau \in [1, 20]$ | $\tau \in [1, 10]$ | $\tau \in [1, 5]$ | $\tau \in [1, 3]$ |
|---|---|---|---|---|
| Obs 1 | 11710 | 6436 | 4994 | 4201 |
| Obs 2 | 10850 | 4686 | 4079 | 3655 |

$x_{i0}$-dependence when $N = 10$, $\tau \in [1, 20]$

| CPEE incl. transients | $x_{i0} = x_0 = 0$ | $x_{i0} - x_0 = -1$ |
|---|---|---|
| Obs 1 | 20470 | 101600 |
| Obs 2 | 16550 | 164500 |

TABLE II

CUMULATIVE POSITION ESTIMATION ERROR AT $t = 600$ SECONDS WHEN $N$, $T_{max}$ AND $x_{i0}$ CHANGES. THE SETPOINT IS ZERO.

## REFERENCES


[1] E. A. Tannuri and H. M. Morishita, "Experimental and numerical evaluation of a typical dynamic positioning system," *Applied Ocean Research*, vol. 28, no. 2, pp. 133–146, 2006.

[2] V. Hassani, A. J. Sørensen, and A. M. Pascoal, "A novel methodology for robust dynamic positioning of marine vessels: Theory and experiments," *Proceedings of the American Control Conference*, pp. 560–565, 2013.

[3] T. I. Fossen and J. P. Strand, "Passive nonlinear observer design for ships using lyapunov methods: full-scale experiments with a supply vessel," *Automatica*, vol. 35, no. 1, pp. 3 – 16, 1999.

[4] M.-D. Hua, "Attitude estimation for accelerated vehicles using GPS/INS measurements," *Control Engineering Practice*, vol. 18, no. 7, pp. 723 – 732, 2010, special Issue on Aerial Robotics.

[5] B. Vik and T. I. Fossen, "Nonlinear observer design for integration of GPS and intertial navigation systems," *Proceedings of the Conference on Decision and Control (CDC'2001). Orlando, FL.*, 2001.

[6] J. A. Farrell, T. D. Givargis, and M. J. Barth, "Real-time differential carrier phase GPS-aided INS," *IEEE Transactions on Control Systems Technology*, vol. 8, no. 4, pp. 709–721, 2000.

[7] T. I. Fossen, *Handbook of Marine Craft Hydrodyamics and Motion Control*. Wiley, 2011.

[8] R. Goebel, R. G. Sanfelice, and A. R. Teel, *Hybrid Dynamical Systems, Modelling, Stability and Robustness*. Princeton University Press, 2012.

[9] M. S. Branicky, *Studies in Hybrid Systems; Modeling, Analysis and Control*. MiT, Cambridge, Masachusetts, 1995.

[10] A. J. Sørensen, *Marine Control Systems, Propulsion and Motion Control of Ships and Ocean structures, Lecture Notes*. Department of Marine Technology, NTNU, 2013.

[11] A. J. Sørensen, "Structural issues in the design and operation of marine control systems," *Annual Reviews in Control*, vol. 29, no. 1, pp. 125–149, 2005.

[12] A. Teel, "Lyapunov conditions certifying stability and recurrence for a class of stochastic hybrid systems," *Annual Reviews in Control*, vol. 37, no. 1, pp. 1–24, 2013.

[13] R. G. Sanfelice, D. A. Copp, and P. Ñañez, "A toolbox for simulation of hybrid systems in matlab/simulink," *HSCC, Philadelphia, Pennsylvania, USA*, 2013.


Preprint submitted to 2014 IEEE Multi-conference on Systems and Control.
Received April 10, 2014.